Role of Biochar as support material for Photo catalytic operation: A Review

Pooja Dhiman, Manisha Dhiman, Arush Sharma, Manita Thakur, Sourav Gautam, Ajay Kumar

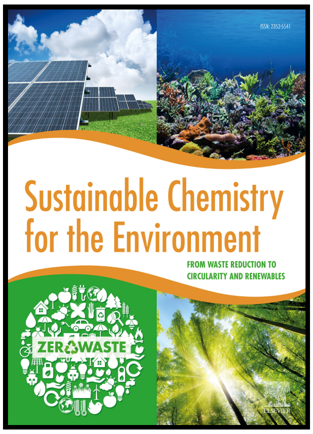

PII: S2949-8392(24)00117-2

DOI: https://doi.org/10.1016/j.scenv.2024.100174

Reference: SCENV100174

To appear in: *Sustainable Chemistry for the Environment*

Received date: 15 August 2024
Revised date: 10 October 2024
Accepted date: 15 October 2024

Please cite this article as: Pooja Dhiman, Manisha Dhiman, Arush Sharma, Manita Thakur, Sourav Gautam and Ajay Kumar, Role of Biochar as support material for Photo catalytic operation: A Review, *Sustainable Chemistry for the Environment,* (2024) doi:https://doi.org/10.1016/j.scenv.2024.100174

Role of Biochar as support material for Photo catalytic operation: A Review

[1]Pooja Dhiman, [1,2]Manisha Dhiman, [3]Arush Sharma, [4]Manita Thakur, [1]Sourav Gautam [1,2] Ajay Kumar*

[1*]Department of Chemistry, School of Basic and Applied Sciences, Maharaja Agrasen University, Solan, (HP), India, 174103

[2]Center of Excellence in nanotechnology, Maharaja Agrasen University, Atal Shiksha Kunj, Solan (HP) 174103, India

[3]School of Sciences, Baddi University of Emerging Sciences and Technology, (BUEST) Solan, Himachal Pradesh, India- 173205

[4]Department of Chemistry, IEC University, Baddi, Solan, Himachal Pradesh 174103, India

Corresponding author: ajaydogra972@gmail.com.

Abstract

Compared to the previous decades, presently the generation of household and industrial waste has increased too many folds. The resulting waste has posed a serious management problem. Various techniques are being explored for organic waste management such as biodegradation, microbial degradation, etc. But still, the processes required technological updates to minimize issues related to cost, ease of implementation, etc. Recently, the pyrolysis of such waste in the limited presence of oxygen is in trend. The product so obtained called as “Biochar” offer immense utilization in the domain of environmental pollutants remediation. Biochar offered varieties of beneficial properties, including high rough, porous as well as high specific surfaces area enriched with various active functionalities. These properties are very beneficial while being utilized as a support material in the Nano regime. The present article consolidates the broad area deployment of biochar in diversified fields including adsorption, photo catalysis etc. A special intention has been given to the deployment of biochar in the field of effluent remediation.

Keyword: Biochar; Photo- catalytic degradation; Waste Water; Remediation; Adsorption;

1. Introduction

The ever increasing population of the world is generating a lot of bio-waste. Anthropogenic activities are mainly responsible for the generation of the domestic and the industrial pollution. **Figure 1** summarizes the different sources of water pollution and its effect on the aquatic and terrestrial ecosystem and their resulting consequences. After rain the land pollution, air pollution transforms itself into water pollution. Not only this, but to greater extent, industrial effluents from the different manufacturing industries is also a major contributor.

In order to reduce pressure on the non-renewable resources, the government of the developing countries has emphasized the researchers of the scientific community to device new strategies to utilize currently being generated waste by converting them into useful products sustainably. The need of the hour is to exercise the novel strategies to come up with feasible solutions with improved efficiency. In order to solve this challenging issue, many traditional techniques had been tried. But majority have their own merits and demerits associated with them for instance lower efficiency, expensive but not applicable on large scale.

The bio mass originating from the organic solid lingo-cellulosic wastes such as agricultural resources, forestry residues, domestic household kitchen waste and wood waste, non-cellulosic animal manure as well as sludge of sewage can be employed as starting feedstock for the synthesis of biochar in a sustainable way [1]. The different sources from which biochar can be prepared are mentioned in **Figure 2**. Bio mass has insignificant physical and chemical features including low bulk density, fibrous nature, and high moisture content, low heating value, high volatile components and relatively greater alkali and alkaline earth metallic portions. Bio mass in the developing countries has always been matter of much concern as waste because such waste has no economic value [2].

The bio mass waste can be utilized as precursor by converting into the stable carbon enriched solid byproduct by combustion of the selected feedstock at temperature range of 200-400°C for two-three hours in the limited supply of oxygen renowned as "**slow pyrolysis"** and the resulting char is renowned as "**Biochar**". At this temperature, the polymeric portions of bio mass generally undergoes sequential degradative chemical transformations, leaving behind biochar with modified peripheral structure and features [3]. Due to the fabrication by slow pyrolysis in the restricted amount of oxygen, a comparatively stable carbonaceous solid by-product so named biochar with highly porous surface, enlarged exposed Specific SA, significant water holding capacity, abundant surface oxygen rich active functionalities and nutrient recycling is obtained, which make it unique support to be used in photo-catalytic systems [4]. Pyrolysis results in the production of three prime products: carbonaceous solid biochar and volatile matter, can later be partially converted into liquid phase bio oil by condensation, and the other “non-condensable” gases such as CH_4, CO_2, H_2 and CO [5]. Depending upon the selected feedstock, bio-mass derived bio-char is proven for its rich mineral content, surface active functionalities , uniformity of pore size distribution, and presents a considerable amount of surface adsorption sites, which enables it to be effectively deployed as an effective as well as efficient adsorbent for the adsorptive mitigation of industrial xenobiotic which are either organic or inorganic from distinct industrial effluents as of textile, paper, agro-chemical and pharmaceutical industry write various fields [6]. Nowadays special emphasize is being paid to the mitigation of polycyclic aromatic hydrocarbons (PAHs) as well as heavy metals using biochar from the environment. As, the formation of biochar with availability of various active functional groups is economically feasible, biochar can be utilized as co-photo-catalyst support for the development of binary/ternary composites in water splitting and carbon-dioxide and hydrogen sulphide capture. Hence the biochar based photo-catalyst composites are being exercised in order to mitigate the hazardous organic contaminants from distinct industrial waste water by adsorption led photo-degradation [7].

2. As clear from above discussion, bio-char is effectively being utilized in variety of applications by different researcher groups. However, the process of synthesis is suffering from the limitation of releases harmful gases (CH_4, CO, NO, CO_2, H_2 and PAHs) and oils to the atmosphere [8]. Hence selection of the chosen feedstock is one of the most crucial decisions to be taken in the very beginning keeping the end application into consideration. The present paper offers an updated review on the fundamental features of synthesis of bio-char by slow pyrolysis, its physio-chemical properties, mechanism of adsorption and photo-catalysis, factors affecting physical properties of bio-char and photo-degradation along with research gaps in the utilization of the bio-char in the different areas of science, engineering, industry and technology. Therefore keeping the applications area and demanded properties of bio-char we have tried our best to consolidate the latest technological updates in term of environmental remediation through biochar utilization [9].**Different Synthetic Strategies for Production of Biochar**

Keeping the required amount of yield of biochar into consideration, here are different types of pyrolysis techniques depending upon the reaction temperature, residence time, heating rate, named as slow pyrolysis, fast pyrolysis and flash pyrolysis, which affect the overall characteristics of the biochar required [10]. Schematic diagram for the magnetic biochar production on the laboratory scale has been depicted in **Figure 3**. Slow, fast and flash as different pyrolytic techniques have different operating conditions and process parametric requirements as discussed below.

2.1 Slow Pyrolysis: Slow pyrolysis, when compared with the other pyrolytic techniques, low temperature and slow heating rate gives greater solid yield (25-35%) over fuel oil and syn gas and improved physio-chemical properties of value added biochar. That is why production of valued product biochar is cheap, effortless and environment friendly with greater solid yields by this process. Pyrolytic treatment of bio mass with high lignin content tends to generate biochar with enormous exposed Specific SA, high fixed carbon content and a reasonably more stable aromatic structure. After pyrolytic process, bio mass has been reported to contain wide variety of inorganic elements that remain in biochar in varying chemical states. The presence of these inorganic elements in different amounts can considerably influence the composition and quality of biochar and the attached functionalities and consequently potential utilization of the produced biochar. Numerous investigations have stated that biochar originated from herbaceous bio-waste have considerably higher amounts of inorganic elemental contents than that of biochar pyrolysed from hard woody bio masses [11]. **Table 1** briefly summaries the different types of biochars prepared from wide variety of types of feed stocks by slow pyrolysis, at definite operating conditions, expressing their extent of porosity as well as BET surface area [12]. The slow pyrolysis is deployed to produce biochar and pyrolytic gas and has the associated merit of relatively greater yield of solid biochar (approximately 40 wt%) with the demerit of generating a relatively low-valued energy commodity i.e. pyrolytic gas with modest heating value [13].

2.2 Fast pyrolysis: In case of fast pyrolysis, the operating temperature above 600°C results percentage yield of char less than 10-30 %. Fast pyrolysis generates some charcoal, mostly aerosols and gas. After cooling followed by condensation, a homogenous deep brown mobile liquid (Bio-fuel) is formed if either wood or low ash feed is used. **Table 2** summaries the biochar prepared from different bio mass materials by fast pyrolysis. Heating the bio mass at quite high heating rates and transference of heat require a finely ground bio mass feedstock of size lesser than 3 mm as bio mass is relatively thermally poorly conductive. Fast pyrolysis is more advantageous because of great deal of detoxification at higher temperature and recovering products of comparatively higher value. At higher temperature, the transformation of aliphatic C-(C/H) into aromatic moieties containing (C-O-C) and CO has been reported to be the prime point for optimizing the aromatization of biochar [14]. Biochar broadly consists of carbon, but, it also consists of some other elements, including hydrogen, oxygen, and other inorganic proportions. Majority of inorganic portions can be restored in biochar synthesized at <500°C. Although, already published literature on thermochemical transformation of bio mass indicated that at least few inorganic species can be transformed or released at the time of fast pyrolysis. While rapid pyrolysis of bio mass at 1300°C, a considerable substantial quantities of alkali as well as alkaline earth metallic elements including K, Na, Ca and Mg can be converted into vapor phase [15]. The synthesis of biochar through fast pyrolysis is primarily aimed at optimizing the production of bio-oil, with solid biochar and pyrolytic gas as lower-yielding co-products. Compared to slow pyrolysis, fast pyrolysis generates a higher-value energy product. However, this process requires a significant capital investment [16].

2.3 Flash pyrolysis: Flash pyrolysis is relatively faster and is supposed to be handling greater volume of feedstock at same volumes of reactor as well as process parameters. Owing to the numerous advantageous features such as greater biochar yield of 60-75%, as a remarkable technology that demands further exploration for energy transformation of bio waste to be deployed as a waste management technique for solids. The prime pyrolysis outcomes of lignin portion of bio waste are phenols. The pyrolysis outcomes of lignin bio waste include phenols, hydroxylphenols, meothoxyphenols and dimethoxyphenols [17]. Yield of oil synthesized by flash pyrolysis can be as great as 60–75 wt% at optimized parametric conditions. For the effectiveness of the flash pyrolysis, temperature, heating rate as well as residence time are supposed to be from 450–600°C, 103−104°C/s and < 1. Flash pyrolytic oil is featured by high water content (usually > 15 wt.). Flash pyrolysis being faster can easily support larger bio waste feedstock volumes at same volumes of reactor and process intricacies. Owing to its advantages of product yield, flash pyrolysis is an considerable technology for the energy transformation of bio waste and can also facilitates as an efficient management strategy for solid waste [18].

Because reaction temperature, time, pressure, heating rate, and initial moisture content of the selected bio mass governs the physiochemical characteristics of the biochar, it is crucial to get the biochar characterizing before its utilization for the mitigation of the target pollutant from the effluent of the target industry. For example, biochar with relatively low Specific SA consequently leading to low adsorptive potential is not favorable for the elimination of the organic/inorganic contaminants from the agrochemical and distinct industrial effluents. Likewise, biochar with high ash content and less carbon content is not recommended for its application in the energy related electric products. Biochar is a more efficient and economic adsorbent for the adsorptive elimination of heavy metals, dyes, pharmaceutical pollutants, agrochemical (insecticides, pesticides, rodenticides, and weedicides) and other pollutants from the other industries because of its pore size distribution properties, greater surface area, adsorption abilities, and more oxygen enriched active functionalities as well as cost effective production. The adsorption potential of the biochar has been reported to be dependent upon the features of the selected feedstock. Such as biochar derived from the sewage sludge, animal dung, living or dead organic (plant) matter is rich in mineral content and considerable amount of adsorption at surface sites [19] . **Table 3** briefly summaries the different types of biochars prepared from different types of feed stocks by flash pyrolysis, at definite operating conditions, expressing their BET surface area, extent of porosity and characteristics. The primary advantage of flash pyrolysis is its significantly shorter residence time compared to slow and fast pyrolysis. Furthermore, the presence of pyrolysis gases in the reaction chamber helps suppress secondary cracking reactions of the resulting products, thereby enhancing the bio-oil yield [20].

3. Factors affecting physical and chemical properties of biochar

Biochar generally demonstrates diversity in its structure; Specific SA (SSA), distribution of pores, surface functionalities, pH, cation exchange capacity concerned physio-chemical characteristics and elemental composition. Effectiveness of biochar characteristics on adsorptive removal of heavy metals because of variations in the starting feedstock, pyrolysis temperatures employed while preparing, and the engineered modification strategy is greatly studied [21]. Biochar's pore structure, governs the SSA for elimination of heavy metals affects the extent of its adsorption potential. Generally, greater exposed Specific SA of biochar gradually results into better adsorption potential. The higher SSA in addition to biochar's greater porosity generally offers greater extent of adsorption active sites as well as the surface charge born electricity decides the extent of electro static interaction between xenobiotic and biochar. The interactions between active functionalities and mineral contents contribute significantly for biochar to adsorb pollutants. Two physical properties, Specific SSA and extent of porosity affect the capability of biochar to adsorptive elimination of heavy metals (HM) and different water pollutants. The size of the pores and the number of pores are also very important for the adsorptive removal of the water pollutants. For example, biochar with smaller sized pores cannot capture bigger pollutant adsorbates irrespective of its polarity or charge [22]. Researchers have already synthesized KOH-engineered biochar synthesized by hydrothermal carbonization (HTC) was investigated for its comparable adsorption efficiency for adsorptive elimination of Cu^{2+} and Cd^{2+} in water with un-modified biochar. The outcomes indicated that the specific SA of engineered biochar was observed to be 2.4 folds more than that of un-activated biochar. On comparison it was indicated that the adsorptive potential of engineered biochar towards Cd^{2+} and Cu^{2+} was remarkably elevated than that of un-modified biochar. As per previously published literature post their targeted engineered modified biochar, the functionalities enriched in oxygen including –O–,–CO–, –COOH and –OH, etc. on the biochar surface get changed [23]. Consequently, the quantity of adsorption active locations for elimination of water pollutants gets raised, thereby upgrading the adsorption capabilities of biochar. The credit of improved adsorptive potential of the modified biochar goes to greater number of –COOH and –OH active functionalities in modified biochar [24]. The dissimilarities in the physiochemical features greatly affect the adsorptive potential of biochar to adsorb water contaminants. Few research investigations have concluded that the chemical features of biochar are more significant than the specific surface area (SSA) in the process of adsorption based removal [25]. Yet, another contributing feature of biochar is surface charge, affecting the adsorptive elimination of heavy metals on biochar surface. Upon utilization of biochar as a support to remove wide variety of pollutants from water, the surface charge of the matrix strongly governed by pH of the matrix. The point of zero charge (PZC) of biochar is the pH at which the net charge on the biochar surface is zero. The pH PZC is strongly influenced by the pH of the surrounding matrix. When the pH of the solution is lower than the PZC, the biochar surface becomes positively charged, favoring the adsorption of anionic contaminants. Conversely, when the pH of the matrix is higher than the PZC, the biochar surface becomes negatively charged, promoting the adsorption of cationic pollutants [26] . Here are the few factors which affect the physical properties of the biochar synthesized by the pyrolytic approach for its utilization as a support as carbonaceous material in the photo-catalytic composite for photo-degradation of target pollutant prevailing in the waste water for the environmental pollutants remediation and has also been illustrated in **Figure 4.**

There are numerous factors such as raw material-surface ion charge, synthetic methodologies-surface charge, pyrolytic temperature-surface active functionalities, surface oxidation-surface basicity, activation of surface-pore structure and SSA etc. that directly or indirectly affect the physical characteristic features of the biochar, the effect of which has been discussed as follows.

3.1 Raw material-surface ion charge: The elemental content of the biochar greatly depends upon the contents of hemi-cellulose, cellulose and lignin portions of numerous bio-waste starting feedstock materials used for its preparation. On general grounds, biochar primarily composed of Carbon(C), Oxygen (O), Nitrogen (N), Hydrogen (H) and other elements, carbon alone constituents greater than 50%. The presence of alkyl groups and aromatic structures consisting of mentioned elements are much significant contributors of biochar. [27] evaluated the elemental composition of biochars originated from wheat straw and manure of pig observed that pig manure biochar is composed of magnesium and calcium on the other hand wheat straw biochar consisting of mentioned elements in considerable amount. Additionally, surface ion-charge, cation exchange capacity, pH and SSA of biochar synthesized from diversified starting raw feed-stocks are also considerably diversified in their features. However, SSA and pore size of the biochar were remarkably impacted by the nature of raw material deployed. For adsorptive removal of Pb^{2+} biochar derived from pinewood demonstrated approximately double adsorptive potential than biochar derived from rice husk [28].

3.2 Synthetic methodologies-surface charge: A large number of previously published literature on experimental research investigations have demonstrated that the adsorption potential of un-modified biochar is narrow as well as demands modification of biochar to optimize its adsorption potential capabilities. The modification techniques had been grouped into two different brackets. First bracket involves the straight engineered/modified raw feedstock deployed for the proffering of biochar and the alternative bracket deals with the engineered/modified of synthesized biochar [29]. For the purpose of modification of starting feedstock, several diversified chemical reagents are deployed to pretreat the starting raw feedstock materials. Contrary to this, original biochar can also be modified by chemical, physical, or deployment of both chemical and physical methods. Engineering of biochar raises its specific surface as well as the quantity and scattering of oxygen rich active functionalities in addition to surface charges can also be modified to optimize the adsorption potential for adsorptive elimination of industrial contaminants from polluted water [30]. Maximum adsorptive elimination performance up to 99.81 % has been recorded through practical engineered modifications strategies. Keeping the specific utilization requirements into mind, it is vital to choose a suitable synthetic and engineering approach to obtain the required physio-chemical features in biochar. Currently, physical activation is the mostly deployed physically engineered modification method, in which, ozone, CO_2, ammonia, or water vapors are utilized as activators. Biochar synthesized from raw materials by high-temperature pyrolytic methods is activated by above mentioned gases for activation, consequently out coming as elevation in the quantity and diameter of holes of biochar, later resulting in an enhancement of the SSA of biochar. Consequently, a more optimized adsorption based performance effect has been illustrated [31]. Microwave radiations as a source of heating is one such suitable example for the generation of meso-pores, reduction in oxygen based acidic functionalities on the biochar surface and subsequent increase in SSA [32]. Chemical modification by nitrogen doping, ultraviolet radiation, organic and inorganic loading, strong base, strong acid or oxidant activation method, is one of the general method deployed to modify biochar. From the experimental based research results on the mechanism of adsorption of heavy metals (HM) and other potential pollutants by biochar, researchers have observed that the characteristic features of biochar can be altered in numerous ways by modifying the features, including the size, modifying the types, pore structure and extent of active functionalities groups on surface of biochar, boosting the SSA by adopting a suitable chemical modification approach [33].

3.3 Pyrolytic temperature-surface active functionalities: Pyrolytic temperature is also observed to impact the biochar properties. Cantrell et al, investigated biochar prepared from widely different variety of animal manure pig, pore structure, turkey, poultry, and cow manure, in pyrolytic temperature between 350−700°C. Researchers reported that the ash proportions of biochar and its pH proffering at higher temperature were relatively more in magnitude in comparison to biochar derived at lower temperature. That is why, to engineer the wide applications, diversified pyrolysis temperatures had been applied and analyzed in the biochar synthesis. The diversified temperatures had significant effect the specific features of biochar [34]. With the elevation in the pyrolysis temperature, the elemental content of Sulphur (S), Nitrogen (N), Hydrogen (H) and related elements in addition to cation exchange potential and number of oxygen rich active functionalities on the surface get reduced. However, the extent of aromatization of biochar get boosted. Additionally, with the elevation in the void structure, the SSA basic nature of biochar and pyrolysis temperature enhances, which is supportive for the adsorptive elimination of metal contaminants. [35] investigated the functionalities in biochar synthesized from the pyrolysis of poplar wood at investigative temperatures. Raman characterization and DRIFTS reported that the carboxyl groups (-COO-) were relatively lesser stable in comparison to the carbonyl groups (-C=O). Ketones and aldehydes functionalities developed at 200° as well as pre-dominated between 300−500°C. Experimental research conducted by [36] investigated the alterations in the SSA of plant biochar and cow manure synthesized at different pyrolysis temperatures and observed that the SSA of biochar enhanced with the elevation in pyrolysis temperature. Generally, biochar proffered by pyrolysis at about 300°C has been reported to be comparatively more enriched with oxygen-containing active functionalities; on the other hand, biochar proffered by pyrolysis at 500−700°C has been facilitated with more enlarged exposed surface area facilitated with micro-pores. The researchers have reported that not only pH but ash content of biochar proffered at higher temperature were recorded to be greater in magnitude in comparison to biochar proffered at comparatively lower temperature. Therefore, numerous deciding factors must be considered during biochar synthesis. **3.4 Surface oxidation-surface basicity:** Generally surface of biochar is facilitated with oxygen-, sulfur- or nitrogen rich active functionalities. Contrary to this, the oxygen enrich active functionalities are quite usual, and can further be classified into basic, neutral and acidic groups depending on their pH characteristics. The acidic groups generally including lactonic, phenolic and carboxyl groups have pH lower than 6. [19] . On the other hand, chromene and pyrone are the most general alkaline functional groups facilitated active sites, whose characteristic features can be owed to the alkaline nature of the carbonaceous exposed surface, which is more prominent in carbon atoms without oxygen because of delocalization of electrons [37]. Sulfur rich active functionalities can modify the adsorptive potential of biochar by altering its pore volume and SSA. The incorporation of nitrogen rich active functionalities can remarkably boosts the polarity of the carbonaceous biochar surface, thereby elevating the specific interaction between industrial water pollutants and polar biochar adsorbents. The surface active functionalities with distinct physio-chemical features interact with the biochar as adsorbent and the liquid matrix keeping their specific structural characteristics into consideration. It has already been declared that the adsorption process of the aromatics is governed by their chemical interactions with the multitudinous surface active functionalities of biochar as adsorbent.

3.5 Activation of surface-pore structure: Not only porosity but SSA of biochar has been recognized as two governing factors in deciding the adsorption potential of poly aromatic pollutants. Thus, augmenting the SSA area and the quantity and diameter of pores are to be engineered for further multiplying aromatics adsorption on biochar. Numerous hole-making techniques had been adopted as activation methodologies for exposing the enormously exposed SSA. More porous structure has been documented to be developed at higher pyrolytic temperature [38]. With elevation in temperature, the unstable proportions in bio mass including hemi-cellulose, starch and lignin after decomposition tend to convert into volatile components including methanol, tar, acetic acid, CO, CO_2 and H_2. The greater proportions of volatile compounds had been recorded to open up the chocked porous cavities and channels to generate structures with greater porosity and makes newly generated greater active sites available. Moreover, distribution of condensed graphene layers on the biochar surface would lead to the development of micro-crystalline structures. The random stacking of graphite clusters also leads to the bigger pore sizes and SSA [39]. Several research analyses have proven that incorporating bio mass accompanied with specific chemical activators had been reported to be remarkably proffered the porosity and SSA and pore volume of biochars. Stronger acids including H_2SO_4, H_3PO_4, and alkalis including KOH, NaOH, and salts had been proved as efficient hole-developing activators; contrary to this, chemical activation by diversified techniques generally outcome in distinct degrees of pore volume and SSA of biochars. From research, it has been observed that KOH as an activator is quite favorable for generating micropores, on the other hand, H_3PO_4 is more supportive for the development of both microporous or mesoporous structures [40]. Attempts have to be taken to enquire the relationships between the pore volume and Specific SA of biochars and the adsorption of pollutants which are aromatic in nature. According to the outcomes of enhanced adsorptive mitigation of dyes pollutant molecules deploying mandarin peel derived biochars with NH_4Cl and $ZnCl_2$ as chemical activation. The SSA about 1085.0 m^2/g associated with volume of pore around ~ 0.194 cm^3/g of MZ-biochar has been reported to be much greater in comparison to those of the M–biochar with SSA about 8.5 m^2/g accompanied with volume of pore: 0.016 cm^3/g and MN–biochar associated with SSA: 181.1 m^2/g in company with pore volume: 0.031 cm^3/g. **3.6 Specific Surface area (SSA):** Biochar'**s** adsorptive potential is governed to a great extent on its number of oxygen rich surface-active active functionalities, SSA, and ion-exchange capacity (IEC). Porosity and SSA of biochar are the governing factors in improving the adsorptive potential of organic pollutants. Thus, enhancing of the SSA, number of pores and diameter of pores are to be engineered for further increasing pollutant adsorption on biochar surface. Because numerous other parameters also impact the adsorption of pollutants by biochar surface and the practical mechanism of adsorption has also been recorded to be complicated, the dominant adsorption elimination mechanism differs from contaminant to pollutant keeping the structural composition and specific characteristic features into consideration. That is why, exploration of the mode of adsorptive removal of metallic pollutants on biochar surface can be better understood only on the theoretical level [41]. According to so far conducted research in this domain, practical adsorption mechanisms including electrostatic adsorption, physical adsorption, ion exchange, complexation, reduction and precipitation. However, the adsorption of metallic pollutants by biochar cannot be credited to an individual mechanism, but rather multiple mechanisms operate for adsorptive removal of contaminants.

3.7 Other factors: Qiu et al, used bagasse, bamboo, peanut shells, and mountain walnut as starting feedstock to synthesize biochar and activate them with chitosan for better and improved adsorptive elimination of the heavy metals (HM) from aqua environment [42]. The elimination of metallic contaminants by adsorption on biochar surface is not only decided by the surface cation exchange capacity, pore quantity, structure and kinds of active functionalities on biochar surface, rather greatly governed by the biochar dosage, matrix temperature, matrix pH, presence of surrounding interfering ionic impurities in matrix, initial concentration of contaminant and nature of biochar exhaustive process and pollutant. Recently, researcher investigated the features of biochar synthesized from waste shells of mangosteen in adsorptive elimination of Cr (VI) from aqueous matrix and investigated the impacts of variable adsorption time, biochar dosage, pH and actuals concentration of Cr (VI) in the beginning. The outcomes of investigation of the adsorption removal, are the evidences of chemical adsorption as a predominant process, facilitated by a pseudo-second-order kinetic model and Sips isotherm [43].

4. Mechanism of adsorption and photocatalysis

4.1 Physical Mechanisms of adsorption:

There are various physical mechanisms into picture to contribute as overall mechanism of pollutants adsorption from the waste water. No single mechanism is whole sole responsible for the elimination of the contaminants by adsorption. Schematic diagram illustrating different physical mechanism for adsorptive elimination of organic contaminants from waste water has been depicted in **Figure 5.** The factors contributing to the overall mechanism of adsorption are discussed below:

(i) **Surface complexation**: Complexation is a process while interaction occurs among electron donors and electron acceptors to generate various concerned complexes. Generally electron donors offer a pair of electrons, whereas organic compounds and metal ions act as electron acceptors. The adsorptive elimination of metal ions, ionic, molecules aggregate among themselves to constitute a reasonably stable and durable newly generated ion through either complexation or coordination reaction. The adsorptive elimination of arsenate deploying composite magnetic Fe-Mn biochar proferred through (direct) pyrolysis of Mn^{2+} and Fe^{2+} ion pretreated bio mass of pinewood (FMM) or simultaneous-precipitation of Mn^{2+} and Fe^{2+} ions on biochar derived from pinewood (FMB) was evaluated by the prominent researchers [44].

(ii) **Co-precipitation**: is another process which makes few specific coexisting soluble materials which can precipitate altogether. The co-precipitation process deals with adsorption on surface embedded and mixed crystal etc. As(V) co-precipitation has been reported as an effective and efficient technique to synthesize biochar impregnated with magnetic Fe-Mn for adsorptive elimination of pollutants from real situation matrix [45].

(iii) **Photo-degradation**: Owing to its enormous biochar's exposed SSA associated with porous structural, morphological features of magnetic biochar, facilitates its deployment as activator of few catalysts for mineralization. Researchers deployed the biochar (magnetic) proffered from peels of banana as an efficient persulfate activator for mineralization of bisphenol A. It was also observed that the encapsulated nanoparticles of γ-Fe_2O_3 improved the photo-catalytic potential of activator persulfate and ~20 mg/L of bisphenol was wholly eliminated in initial 20 minutes by the promising magnetic biochar. While the mineralization photo-degradation of bisphenol, the oxidative photo-degradation mechanism by involvement of superoxide and hydroxyl radicals contributed significantly [46].

(iv) **Ion exchange**: In order to adsorb few inorganic impurities as ions from the solution, ion exchange process is very commonly employed. The unit operation deals with the separation engaged in mass transfer process. Likewise, ion exchange is a potential reversible reaction accountable for exchanging ions equivalently. Researchers evaluated mechanism of adsorption of $Cd^{2+ \text{ and}}$ Pb^{2+} ions from waste aqueous matrix deploying sulfonated nanoparticles (magnetic) composites as adsorbents. The XPS and FTIR data have revealed that cation exchange technique has been an acceptable approach for extraction of heavy metal on exposed surface of sulfonated biochar (magnetic) nanoparticle. Therefore, the sulphur loaded binding sites on the outer magnetic biochar surface permitted the development of heavy metal ion complexes remarkably boosting the adsorptive elimination potential and capacity of concerned biochar(Magnetic) [44].

(v) **Electrostatic interaction**: Includes both electrostatic repulsion as well as electrostatic attraction to build either electrovalent or chemical bond. By experimental evaluation of the adsorptive elimination of Cr(VI) and As(V) from aqueous matrix deployment of modified or engineered biochar as adsorbents, indicate the prime mechanism for adsorptive elimination of Cr(VI) as well as As(V) possibly be the electrostatic interaction among numerous the pollutant molecules to get adsorbed and the modified/engineered surface of biochar [47].

(vi) **Chemical bond adsorption**: It involved in a comparatively strong chemical interaction among two or more adjoining atoms or ions in a crystal or molecule. As per the outcomes of experimental investigations on the adsorptive elimination of arsenate on magnetite-treated biochar derived from water hyacinth, the practically possible mechanism of adsorptive elimination of As(V) had been reported to inter-change pollutant As(V) molecule with Hydrogen bonding at the hydroxylated exposed Fe_3O_4 surface [48]. XPS investigations further evidenced the prime existing form of arsenic As(V) pollutant adsorbed on magnetic biochar's surface. In the investigations of Pb(II) elimination by treated biochar, has evidenced that mechanism of adsorptive elimination was not only restricted to the involvement of manganese oxide (MnOx) loaded nano-sized particles and existed oxygen-rich surface active functionalities but and π-π* transitions and prevailing vacancy defects also impacted the adsorptive elimination process [49].

(vii) **Reduction:** In the systematic and careful research investigation of Pb (II) adsorptive remediation plausible mechanisms, was observed that the reduction mechanism had contributed significantly in elimination of Pb^{2+} by magnetic biochar derived from sludge [50]. Yet in other research had demonstrated that reagent Ferric Chloride ($FeCl_3$) boosted the extent of porosity of composite magnetic carbon, primarily because of the strong plausible reduction reaction among molecules of iron oxide (g-Fe_2O_3 and Fe_3O_4) and amorphous form of carbon [51].

(viii) **Physical adsorption:** The Interaction primarily takes place among pollutant molecules and available active functionalities of magnetic biochar. Furthermore, available active functionalities contribute prominently in oxygen loaded active active functionalities associations to eliminate pollutants from water matrix. Researchers evaluated the synthesis, modern characterization and adsorptive elimination mechanism of Cu(II) from aqueous matrix by MnO_x-loaded biochars [52]. The adsorptive elimination capacity of Cu(II) on surface of MnO_x-loaded precursors was primarily depends on the development of MnO_x and oxygen containing active functionalities on surface of biochar. Additionally, several mechanisms including pi-pi bond and cation exchange had also been involved in adsorptive elimination of Cu^{2+} [53]. After investigating plethora of previously published literature, it can be concluded that ion exchange, electrostatic interactions and surface complexation in addition to oxygen enriched active functionalities are the preferential mechanisms for adsorptive elimination of heavy metal (HM) contaminants on surface of magnetic biochars.

4.2 Mechanism of photo catalytic degradation and mechanism of adsorption cum photo catalytic degradation

Plethora of published literature prove that advanced oxidation processes (AOPs) are quite effective techniques for carrying out oxidation and degradation of variety of inorganic and organic pollutants that are not degradable by traditional techniques. In-situ intermediate reactive oxygen species (ROS) had been reported to get produced in advanced oxidation Processes (AOPs), primarily the hydroxyl free radicals which accelerate the process of degradation until the targeted pollutants are fully transformed into non-hazardous simple inorganic acids, H_2O and CO_2 [54]. In few reactions, non-toxic salts can also be mineralized, but that depends completely on the nature and composition of the specific pollutant. Numerous different combinations of hydrogen peroxide, ozone, ultraviolet (UV) radiation, sonolysis and photo-catalytic treatments are used in AOPs, which are able to oxidize variety of pollutants present in air, soil and water [55]. In last few decades, only few selective AOPs had been adopted for environmental pollution remediation applications. Some of which are ozonation, catalytic peroxidation, semiconductor photo-catalysis (using ZnO and TiO_2), Fenton reactions systems, sono-photo-catalysis and sonolysis [56].

Researchers of the scientific community reported that advanced oxidation processes (AOPs), which use potent oxidizing agents to degrade organic pollutants, had been identified as viable strategy for wastewater treatment. Photo-catalysis has been broadly deployed in treatment of waste water since the initial report of TiO_2 photo-catalytic oxidation under ultraviolet light (UV) [57]. While the light transmittance is required to be taken into account in practical waste water treatment, photo-catalysis is a "green" disinfection approach that uses clean and green solar energy and is carried out under mild conditions. Reactive oxygen species (ROS) of various types including hydroxyl radicals (•OH), singlet oxygen (O_2), and superoxide radicals ($O^{2\bullet-}$) are to be produced when photo-catalysis is stimulated [58]. Main disadvantage of the use of excess photo catalysts causes agglomeration due to their higher surface energy. Biochar has high, porous surface energy facilitated with wide varieties of oxygen rich active functionalities for anchorement of the nanoparticle. Thus, biochar behave as good support for nanoparticles [59]. Practical applications of photo-catalysis are its operating cost, sustainability, low ROS generation efficiency. Need for large surface area for visible light harvesting due to their narrow band gap allow $e^- h^+$ coupled pairs to form with even lower photon energy and thus, semiconductors based on silver, bismuth, tin, carbon and quantum dots can be triggered by visible light [60]. In photochemical reaction, reactive oxygen species can be generated by activation of oxidants or water molecules [61]. **Figure 6** depicts the general schematic diagram for mechanism of the photo-catalytic process.

Previously published literature has evidenced that pollutants can be removed from water by using adsorption cum photo-degradation technique. **Figure 7** represents brief description of the adsorption process.

4.3 Mechanism of adsorption led photo-catalytic degradation Process:

In the adsorption led photo-catalytic reactions, reactive oxygen species (ROS) are generally generated between sensitive substances present in the environment or by catalytic enzyme activities undergoing within living organisms. Hydroxyl free radicals hydrogen peroxide (H_2O_2), (·OH), superoxide anion radicals ($O^{2-\cdot}$**)** and singlet oxygen ($^1O_2$) are some others are examples of typical ROS. O_2 and H_2O_2 are generated by oxidizing or reducing H_2O, respectively [62]. Hydrogen peroxide can be reduced further by break down of the bond between O-O bond for formation of OH free radicals and O_2 can be oxidized for production of

O_2. Semiconductor nanoparticles are photo-excited by light irradiation (either UV or visible light) in conditional photo-catalysis. When photon energy of a semiconductor's band gap is larger than or equal to that of the photon, photo-induced electrons are driven to the conduction band (CB) to generate electrons with high reductively, leaving holes (h^+) with high oxidizing capacity in the valence band [63]. When photo-generated e^- and h^+ couples combine inside a semiconductor, either light or heat is released. Separated carriers of charge will then transferred to the surface of the catalyst and take part in surface redox processes. On the exposed surface of the excited photo catalyst, H_2O is oxidized to generate HO free radicals during the process and dissolved O_2 can be reduced by an excited electron to $O_2^{\bullet}$ [64]. Illustrated diagram depicting the brief mechanism of adsorption led Photo-catalytic Process is demonstrated in **Figure 8**.

According to Qin et al, initially, the fabricated composite is supposed to get excited in the region of visible light because of its tunable band gap associated with about ~ 2.84 eV of energy. Consequently, the photo produced electrons (e^-) are translocate to the conduction band (CB) of g-C_3N_4, and the positively charged holes (h^+) are left vacant in the valence band (VB) [65]. At later point of time, owing to the electron acceptance characteristic features of biochar, the electrons had been documented to be captured immediately by the biochar and discharge to the photo-catalytic surface subsequently reacting with surrounded oxygen (O_2) to produce superoxide free radicals ($O^{2-\cdot}$) [66]. During this time, h^+ from the valence band (VB) of g-C_3N_4 are capable enough to directly encapsulate H_2O to produce hydroxyl free radicals (·OH). The rationale behind all this is that more is the negative valence band (VB) edge potential, so hydroxyl free radicals ($^{\cdot}OH$) generated via mentioned route. The hydroxyl ($^{\cdot}OH$) and superoxide ($O^{2-\cdot}$) free radicals are important active species and positively charged holes (h^+) are also the main active chemical species. That is why both the radical generated, reacts directly with organic pollutants to generate non-toxic and non hazardous small inorganic molecules including carbon di oxide (CO_2)and water (H_2O) and h^+ has the potential to directly oxidize the organic contaminant [67].

5. Applications of biochar for environmental remediation: The previously published studies have reported the evidences of potential applications of biochar as an adsorbent and as inert carbonaceous support for the photo-mineralization of the water contaminants in environment pollutants mitigation. As adsorbent, biochar has proven records of adsorption of wide variety of heavy metals from the effluents discharged from the textile, leather, agrochemical, packaging, pharmaceutical and other personal care products industries. Furthermore, applications of biochar had been summarized as sole adsorbent for adsorptive elimination of water pollutants and then biochar as an inert carbonaceous support for adsorption cum photo-degradation of the organic waste water pollutants.

5.1 Removal by adsorption: Aqueous pollution is one of the major global concerns that are affecting the health of biotic community through each component of food chain. Day by day demand for the clean water for the various human activities is increasing. Hence the waste water management has become a global responsibility. Different water treatment techniques including filtration, adsorption, ion-exchange as well as degradation are currently being employed in the industries for waste water remediation. Treasure of literature is claiming that 99% of some specific pollutants can be eliminated from the waste water at certain idealistic conditions of specific pH, pollutant concentration and other operating parametric conditions [68]. Adsorption process had been an effective, economic, efficient method to mitigate heavy metal (HM) ions and other pollutants from aqueous environment because of its convenient utilization, high efficacy and cost effectiveness. Previously published studies have shown that biochar made from waste root of malt, sago from the cassava plant, and coconut shell fiber can effectively remove variety of pollutants from aqueous solutions [69].

5.1.1 Biochar for adsorptive removal of Heavy Metal Pollutants: The researchers succeeded in elimination of greater quantities of macronutrients (alkaline earth metals eg. Ca, Mg and alkali metal K) and comparatively lower quantities of metals (Cd, As, Pb, Cr, Cu and Zn) owing to the macro-porous biochar structure and micro-porous structure of granular activated carbon along with life cycle benefits on packed bed columns. For the removal of pollutants on porous biochar surface along with the oxygen rich active functionalities offered a good capacity to retain copper due to combined effects of adsorption, precipitation and co-precipitation process, which are governed by the physic -chemical features of the bio mass feedstock as precursor and the resultant biochar itself [70]. The upper limit of adsorptive potential of modified sugarcane baggage derived biochar for elimination of nitrate ions from aqueous matrix by adsorption was obtained as 28.21 mg/g. Nitrate ion elimination by adsorption was reported efficiently higher under acidic pH in comparison to basic pH which might be because of reasonable electrostatic forces between the modified biochar surface and nitrate ions with achievement of adsorption equilibrium within 60 min with pseudo-second-order kinetic model and Langmuir isotherm model. The cost effective elimination of metal ions including cadmium (Cd^{2+}) and lead (Pb^{2+}) with waste products derived biochar by kinetics and adsorption mechanisms from soil is potential technique [71]. The adsorption capacities of biochar increased after alkaline treatment for elimination of Cd^{2+} and Pb^{2+}. Optimum adsorption capacities were recorded to be about 68.08 mg g^{-1} and about 175.53 for cadmium (Cd^{2+}) and lead (Pb^{2+}) respectively. The pseudo second kinetic equation and Langmuir adsorption isotherm supported the adsorption processes, evidencing the adsorption mechanisms of Pb^{2+} and Cd^{2+} by biochar are complicated and preferentially regulated by chemical adsorption. Due to hydrolysis of lead (Pb^{2+}) at relatively lower pH values, biochar has more attraction for Pb^{2+} in comparison to Cd^{2+}. The elimination of Cd^{2+} and Ni^{2+} for adsorptive competition on the porous surface of rice straw originated biochars proffered at 700°C (RB700) and 400°C (RB400) accounted for about 60% and 36% of the adsorptive potential respectively. Using biochar as the adsorptive support, type and the concentration of the ions are taken into consideration when targeting the elimination of metals from the soil or water. Cadmium (Cd^{2+}) had been recorded to be in competition with Ni^{2+} for available binding sites at actual reported concentration of metal pollutants greater than 10 mg/Lfor RB400 and higher in concentration than 20 mg/L for RB700. The adsorption sites for Ni^{2+} and Cd^{2+} and on the biochar surface were recorded to be greatly intermixed and the attaching of Ni^{2+} and Cd^{2+} to these functionally active sites was influences and directed by the order of occupancy of these available active sites by the pollutants metals. For adsorption of Ni^{2+} and Cd^{2+} on the binary system, cation exchange mechanism and precipitation mechanism had been documented as the prominent mechanism of adsorption on RB700 as well as RB400, respectively. The outcomes of competition had declined the contribution of cation exchange but raised that of precipitation. Researchers found that Cu (II), Zn (II), Cd (II) and Pb (II) strongly adsorb on pig and cow manure proffered biochars at 400°C. Their sorption percentage rose with the rising initial quantities of Metal (II) ions. The factors affecting adsorption process are number and size of particle, concentration of solutions, pH, and temperature and phase contact time. Maximum elimination of these ions was reported at pH in the range of 5–6. The kinetics of adsorption process had been observed to be well supported by the model of pseudo second order. The diffusions of intra particle was one of the rate limiting steps of the adsorption elimination process [72]. **Table 4** corresponds to the adsorptive elimination of heavy metals on the biochar surface. Electrostatic interaction and ion exchange dominate for the adsorptive elimination of Cr (VI) adsorption on biochar surface under acidic pH conditions. Cr (VI) ions tend to degrade into CrO_4^{2-}, $Cr_2O_7^{2-}$ and $HCrO_4^{-}$ ions in water environment. At relatively lower pH (~1–4), presence of $HCrO_4^{-}$ ions corresponds to the electrostatic interactions owing to the availability of active active functionalities including $-OH_2^{+}$, $-NH_4^{+}$ and $-COOH$ groups supporting improved adsorptive removal of Cr (VI) as pollutant. Equilibrium isotherm, thermodynamic kinetic models assist to better correlate the Cr(VI), the involved mechanisms for biochar interactions as well as their adsorption removal [73].

5.1.2 Biochar based adsorbents for removal of the agrochemicals: From agricultural sector, a great number of chemicals being used in farm lands in order to protect the crop from the moths, insects, rodents, pests etc. are being discharged in the natural water bodies after the fulfillment of their targeted utilization. Bentazone is a commonly used toxic insecticide to limit gypsy moths, boll weevils, forest tent caterpillar moths and several other kinds of moths in various farm lands. [74] observed the efficiency of biochar synthesized from bio-waste of Azardirachta Indica by pyrolysis in restricted supply of oxygen as adsorbent for elimination of Bentazone. The outcomes of experimental investigations adsorption parameters at pH 8, were observed to be with150 min of equilibrium set up time, with 0.5 g of biochar. The outcomes of the optimization investigations, pH 2, with 0.952 desirability was achieved with 79.40 mg/g as adsorptive uptake and for 50 mg/L of initial insecticide concentration with 0.448 g dose of adsorbent for 30 min contact time. As per study, the data of adsorption isotherm for the elimination of Bentazone well matched with the Freundlich isotherm. The outcomes of the investigation revealed that the biochar proffered from the Azardirachta Indica bark as bio waste can efficiently be deployed as a potential promising adsorbent for elimination of organic xenobiotics from aquatic matrix. Researchers [75] conducted studies on adsorption of imidacloprid (IMIDA), atrazine (ATZ), as well as azoxystrobin (AZOXY) in sole-, di- as well as ternary-pollutants deploying phosphoric acid-modified biochar derived from rice straw (T-RSBC). The T-RSBC demonstrated powerful and more improved adsorption capability potential for IMIDA in sole- and di-pollutant matrix systems. Freundlich constant (KFads) in ternary matrix system follow sequence as follows: AZOXY (~1459)> IMIDA (~1314)> ATZ (~222.7). Molecular dynamics and Adsorption modeling had already evidenced that non-bonding interactions among diversified aromatic groups and ongoing electrostatic interventions associated with the phosphate ester group in T-RSBC contributed remarkably. The improved adsorption because of pore-filling can be attributed to the layering of pesticide molecules as pollutant as if multi-stacked. IMIDA was preferentially adsorbed through mechanism of pore-filling, on the other hand, ATZ adsorbed by mechanism of partitioning. According to the studies the percent elimination of the three pesticides as pollutants from waste eluent water followed the sequence as ordered: AZOXY > IMIDA > ATZ. Isotherm Freundlich supported multifactorial Sheindorf- Rebuhn- Sheintuch (SRS) equation’s recommended that the degree of adsorption of ATZ, in the co-existence of co-existing pesticides as pollutants, reduced with rise in number of pollutants as per order (KiATZ, Ternary < KiATZ, Binary < KiATZ, Single). Competitive coefficient magnitudes (αATZ/IMIDA, Ternary > αATZ/AZOXY, Ternary) indicated that ATZ adsorption in ternary system was limited greatly by the availability of IMIDA in comparison to AZOXY [76]. The outcomes of the evaluations recommended that biochar associated with a greater non-carbonized fractional phase supported non-competitive adsorption. According to the research conducted by the researchers of [77], the exposed surface area, carbon content and the aromaticity of the biochar derived from peanut shells increases with increasing prolytic temperature for the adsorptive removal of pesticide imidacloprid. The adsorptive elimination of imidacloprid was an endothermic process and adsorptive potential was increasing with increasing temperature. Not only this but the temperature of the effluent also supported the sorption of the pesticide on the biochar PB700 and the adsorptive elimination rate also rose by PB700 with greater pH in acidic and neutral conditions. Kinetic models pseudo first order and pseudosecond order, matched well the adsorption kinetics of imidacloprid on PB700 surface. The researchers of [78], synthesized the carbonized biochar (BC1) proffered from coconut shell, activated biochar proffered from (BC2) coconut shell, chemically (BC3) modified phosphoric acid biochar and sodium hydroxide treated (BC4) coconut shell biochar for the adsorptive elimination of pesticide diazinon as pollutant molecule. The outcomes of the investigational research concluded that the characteristic features of biochar through EDX, SEM and BET analytical evaluations indicated the more porosity of intricate surface morphological features and slight alterations in the association with enormous exposed surface area (~405.97 – 508.07 m^2 /g) by following the order BC3 > BC2 > BC4 [79]. The analysis indicated elimination of diazinon at neutral pH 7 as high as 98.96% with BC3 with 5.0 g/L adsorbent dose. Great R^2 coefficient of determination, with a shorter magnitudes of ERRSQ and associative error χ^2 analysis generally offers the BC2 (~0.9999) and BC1 (~0.9971) best matched with isotherm Freundlich revealing multilayer adsorption on the heterogeneous surface contrary to this, model Langmuir isotherm had previously been documented to be the best matched to elaborate the monolayer adsorption on the homogenous surface of both biochars BC4 as well as BC3. The outcomes hinted that maximum adsorptive potential (qm) was obtained by biochar BC3 with ~10.33 mg/g, subsequently followed by biochar BC2 (9.65 mg/g) according to isotherm Langmuir on the other hand isotherm Freundlich revealed the greatest adsorptive potential (kF) with ~1.73 mg/g $(L/mg)^{1/n}$ later followed by biochar BC4 with ~0.63mg/g $(L/mg)^{1/n}$ at supportive and favorable adsorption isotherm ($1 \leq n \leq 10$) [78]. Thus, the evaluation outcomes so received indicated that both biochars BC2 as well as BC3 are more efficient adsorbents and had demonstrated higher adsorption capacity in eliminating diazinon from aqueous matrix.

Nayak et al, has conducted a comparative investigation on the five types of biochar proffered from agricultural bio mass wastes based, bamboo chips (BCBC), rice straw (RSBC) acid treated RSBC (T-RSBC), corn cob (CCBC), eucalyptus bark (EBBC) and rice husk (RHBC) for evaluating their physio-chemical characteristic features and adsorption pattern of imidacloprid and atrazine as pollutant molecules. The kinetics study carried out by the researchers revealed that excluding atrazine adsorption on RSBC, was most supported by model pseudo second order, adsorption of atrazine and imidacloprid on biochars surfaces was supported by the modified model Elovich. Out of the five biochars, the RSBC expressed the maximum ~39.9–77.8% imidacloprid adsorption and removal of atrazine ~37.5–70.7% adsorption [80], [81]. Contrary to this, biochar treated by phosphoric acid RSBC later boosted the adsorption of both pesticides pollutants in T-RSBC assembly. The isotherm Freundlich adsorption were considerably nonlinear and percentage of adsorptive elimination reduced with rise in the concentration of pesticide as pollutant in the aqueous matrix. Adsorption of pesticide on surface of biochars was impacted by their polarity, aromaticity, weak acid fraction, pore diameter and experimental pH conditions. Furthermore, results revealed that rice straw biochars have considerable adsorption capability and potential for environmental elimination of pollutants and can be deployed as adsorbents for elimination of pesticides imidacloprid and atrazine as agricultural contaminants released from agricultural industry in the discharged waste water bodies [82]. The surface of biochar had been observed to retain water-soluble arsenic (As) on its surface during the investigation [83]. A boost in temperature had been observed to decrease the adsorption of Hg by biochar derived from brazilian pepper from 24.2 to 15.1 mg g^{-1}. Adsorptive potential of brazilian pepper had been reported from 23–31 and 69–77% at 300 and 450°C respectively [84]. The working mechanism in case of adsorption of Hg by biochar originated from brazilian pepper has been reported to be highly associated via complexation with carboxyl, hydroxyl and phenolic groups [85]. Adsorption of Hg by complexation with thiol groups had also previously been observed via X-ray analysis [86]. Adsorption of organic contaminants through partitioning mechanism had been reported to be dependent upon the characteristic features of carbonized forms such as graphene and its other crystalline versions and non -carbonized forms including non-crystalline, organic carbon and amorphous forms of biochar [66]. The initiation of partitioning mechanism takes place either by diffusion of adsorbate into the pores of organic matter or non-carbonized fractions of biochar [87]. In the later phases of adsorption, in partition mechanism, the target organic pollutants get solubilized in the bulk of organic contents of biochar with the agenda to increase their adsorption. In biochar, partitioning of organic contaminants has been observed to takes place occurs at the carbonaceous amorphous fractions rich in the aliphatic and poly aromatic compounds including phenols, sugars, and ketones etc [67].

5.2 Removal of pollutants by adsorption cum photo catalytic degradation

Since years, biochar has demonstrated significant potential in the mitigation of industrial pollutants from waste water. The rationale behind using biochar as a support material for photo catalytic mineralization of organic pollutant dye is the improvements of the catalytic potential of biochar by, high temperature treatment, acid treatment, metal loading and doping with heteroatom had been proven to be the efficient approaches [88]. Approximately all modification techniques improved the adsorptive capacity of the biochar by altering the specific active functionalities loaded biochar structure and oxygen-enrich active functionalities, persistent free radicals (PFRs), defects and porous structure are the primary indicators that had been documented previously. Although, the specific contribution of diversified characteristic features of biochar is yet to be studied in detail [89]. **Figure 9** Refers to the photo-mineralization of the organic contaminants by diversified biochar based photo catalyst. Researchers concluded that the extent of porosity in the structure of biochar can be altered by the addition of reagents like ferric chloride ($FeCl_3$) during synthesis of biochar. Investigation of biochar treated with Fe-Mn binary oxides raised the catalytic efficiency of biochar. Post-loading of the Fe-Mn binary oxides on surface of biochar, the mineralization of naphthalene rose from 44.9% to 82.8% within 148 minutes [90]. The credit of this goes to a rise in the number of generation of active free radicals can potentially act as active sites in the systems such as Fenton system. Additionally, the Fe-Mn binary oxides inculcated magnetism in biochar. Hence, research investigated metal loaded biochar simultaneously to endure magnetism and enhance the catalytic efficiency [45].

5.2.1 Removal of pollutants from waste water

The recent studies declare the ever increasing industrialization as the prime cause of the contamination of water by organic dyes, paints, insecticides, pharmaceuticals and others [91]. Treasure of literature in this fields has been documented with the use of carbonaceous nanotubes, carbon dots and graphene for the elimination of dyes and brominated flame retardants these contaminants from the waste water [92]. Despite of being so efficient, the high cost of operation has restricted the usage of theses carbonaceous materials in the real time for the removal of the organic xenobiotic from the real situation matrix. The removal of these organic pollutants from the water at the oxygen rich active functionalities with macro-porous biochar surface can be due to strong electrostatic hydrophilic (Hydrogen bonding/pi-pi orbital interactions) is a cheaper solution [93]. But keeping the nature of the organic contaminants and biochar active functionalities in considerations, these interactions can be hydrophobic interactions too. The synthesis of municipal solid waste derived biochar at 450°C for 30 minutes in an onsite pyrolyzer for the elimination of volatile organic pollutants m-xylene and toluene. Langmuir adsorption potential capacities were reported as great as 850 and 550 $\mu g.g^{-1}$ for toluene as well as m-xylene respectively [94]. As per the authors, the apparent rate of adsorption of phenanthrene remarkably rose when biochar with relatively shorter particle size was deployed. By deploying the model of principles of intra-particle diffusion, a strategy to investigate the radius of an individual biochar particle, represented as particle radius (RZ) that expressed the size-dependent rate of adsorption. A moderate correlation as linear among the normalized apparent rates of adsorption determined from experimentally received data and the inverse square of RZ is recorded for rice husk, wood chip and sewage sludge derived biochar at 250-500°C. The kinetics of phenanthrene adsorption on the biochars is well elaborated by the model of intra-particle diffusion with remarkable greater rates of adsorption as demonstrated by finely grained biochars. Total time taken to reach 95% of equilibrium for adsorptive elimination of phenanthrene on biochar is declined from ~4.6–17.9 days in comparison to the original biochars to <1–4.6 days for the <125 μm sized powdered biochars [95]. According to the scientists, no competition (t-test, $P < 0.0001$) ha been recorded among α-, β-, γ- and 27 δ- isomers of hexachlorocyclohexane's (HCH) from water on three biochars synthesized from, greenhouse tomato bio waste (550ºC), durian shell (400ºC) and digestate (700ºC). Freundlich adsorption constants of α-, γ- and δ-HCH followed the sequence: BC durian shell < BC greenhouse tomato waste <BC digestate in comparison to β-HCH which followed the order: BC digestate < BC greenhouse tomato waste <BC durian shell. Factors iron content and surface area in addition to hexachlorocyclohexane (HCH) - Biochar matrix interactions affected the adsorption coefficients most strongly [96].

5.2.2 Removal of Dyes from waste water

According to the literature, polysulfone intermixed matrix hollow fibrous membrane (MMM) or micro-scale biochar particles demonstrated high elimination efficiency of dye methylene blue as a pollutant from a wide pH of 4 to 10 in the waste water. The adsorptive remediation of contaminant dye molecule on MMM and biochar surface followed the Langmuir isotherm and model intra-particle surface diffusion. At neutral pH, for MMM, the optimum adsorptive potential was 165.808 $mg.g^{-1}$and for biochar recorded was 544.459 $mg.g^{-1}$. In case of MMM, the adsorption equilibrium was recorded to be set up within 8 h and nanoparticles of biochar, take 4 h respectively. At pH 8.0, the optimum adsorptive potential of methylene blue had been recorded as 544.459 mg.g^{-1} for biochar particles and 165.808 mg.g^{-1} for MMM. Electrostatic interaction, hydrogen bonding, pi-pi orbital interactions and hydrophobic interaction contributed significantly in the adsorptive elimination of methylene blue from the water [97]. Biochar derived from hydro char pyrolysis of bamboo shoot shell at with 800°C as temperature of pyrolysis demonstrated with well-structured pores with 513m^2/g of surface area. The optimum adsorptive elimination potential of rhodamine B (RhB) at 25°C on BHC-800 surface has been recorded to be 85.8 mg.g^{-1}with isotherms matched well to model Freundlich. The biochar's micro-structure had been observed to get altered significantly with temperature, and adsorptive remediative performance for rhodamine B (RhB) at diversified temperature 0°C, 25°C and 40°C were investigated by the researchers in depth. The time taken for set up of adsorption equilibrium in case of RhB on BHC-800 biochar surface was recorded to be about 20 min with the received data matched improved to the pseudo-second-order kinetics for the efficient and effective adsorptive remediation of RhB dyes as pollutant from contaminated water. According to the literature, the lowest temperature of 0°C was recorded to favor the adsorptive removal of RhB on BHC-600 as well as BHC-300 surfaces whereas the temperature of 25°C favors the adsorptive elimination of RhB dye as contaminant on the BHC-800 surface because of varying pore structure and doping of surface groups [98]. Biochar synthesized from pecan nutshell was characterized to explore more of its features, and deployed as an option, economic and cost effective adsorbent for elimination of textile pollutants molecule Reactive Red 141 (RR141) as xenobiotic from waste water matrix. The yield derived from biochar extracted from raw pecan nutshell was documented about 30%. The biochar presented a micro or meso-porous structure with 93 m^2.g^{-1} surface area, which is considered great for bio waste derived bio mass materials. For both, raw pecan nutshell and the biochar derived from it, the RR141 adsorption was supported under acidic pH of 2 and 3, respectively. Elimination percentage of RR141 was 85% deploying the biochar as an efficient adsorbent, and was recorded to be only 23% in case when sole biochar derived from raw pecan nutshell had been deployed. As per published literature, the adsorption kinetics for adsorptive elimination of contaminant RR141 on the biochar surface suited matching with the model pseudo second order kinetic. As per the received experimental data, the equilibrium isotherms were well elaborated by the Freundlich model. The optimum adsorptive elimination capacity was reported to be about 130 mg/g. The findings indicate that adsorption was favorable, exothermic and spontaneous. These outcome demonstrated that the new biochar prepared proved to be an alternative, cost effective, and ecofriendly adsorbent that has potential to eliminate dyes from colored effluents [99]. Not only was this but magnetic biochar/Fe_3O_4 Nano-composites (M-BC) from marine macro algae deploying a facile electro-magnetization strategy deploying a stainless steel electrode-supported electrochemical assembly, led by fabricated pyrolysis. Chemical as well as physical analysis demonstrated that the porosity in addition to magnetic characteristic features were parallel upgraded through the electro-magnetization procedure strategy, enabling comparatively greater adsorptive performance, but at the same time also facilitates easy separation or recovery from aqueous matrix at after adsorptive elimination deploying a bar magnet. The adsorptive elimination equilibrium results, Sips model efficiently estimated the potential adsorptive potential, documented to be 382 mg/g, 297 mg/g as well as 190 mg/g at 30, 20 and 10°C respectively. The recorded observations indicated considerable performance of the biochar with significant porosity and magnetism to efficiently remove acid orange 7 from aqueous matrix [100]. However, in the real practical scenario, the efficiency of remediation of different pollutants by different techniques is decreases substantially. **Table 5** corresponds to the utilization of biochar photo catalysts in removal of dyes from waste water discharged from textile industries. Hence, in practical scenario adsorption cum photo-degradation has claimed to mitigate both organic and the inorganic pollutants [80].

5.2.3 Removal of phenolic compounds from waste water

According to the literature, bio mass-derived adsorbents are more in demand in comparison to chemical supported for the elimination of crude oil spillage in water bodies of marine ecosystem because bio mass-derived adsorbents are more eco-friendly. Peat-derived biochar has been evaluated as bio-adsorbent for the adsorption as well as elimination of spilled crude oil from simulated sea water. The optimum crude oil adsorption potential by target biochar and percentage oil elimination efficiency was reported to be 32.5 g of crude oil per gram of adsorbent in addition to 91.2% respectively. Optimum adsorptive elimination values were assessed after 70 min of contact of biochar-crude oil inter-mixing time, at 45°C. The spent adsorbent retained its adsorption potential even after three cycles of regeneration and reusability, indicating that the novel composite can still be reused [101]. Biochar (BC) pyrolysed from the pine wood gasification was investigated for the adsorptive elimination of toluene from water and its potential adsorption capability was later compared with activated carbon (AC). Biochar is characterized by high and faster toluene elimination in comparison to AC. Morphological and textural analysis revealed that the extent of porosity of activated carbon (AC) is two folds in comparison to biochar (BC). Equilibrium investigations indicated that the sorption ability of biochar can be compared with that of activated carbon (AC), so the material's extent of porosity is one of the parameter which decides adsorptive elimination of toluene. Potentially recorded specific adsorption performance in terms of mg adsorbed/m^2 of surface of the biochar is greater in comparison to that of activated carbon (AC): toluene has been recorded to be highly adsorbed on biochar surface. Biochar pyrolysed from pine wood gasification biomaterial offers deployment of biochar economically and environmentally convenient in comparison to activated carbon (AC), which, as a synthetic adsorbent, manufactured in controlled laboratory conditions for a target application. For the purpose of comparison of potential adsorption capabilities of the BC to that of AC, recorded and noted SSA 343 and 712 and m^2.g^{-1} for BC and AC for deionized and synthetic seawater respectively. Exposed surface area and total pore volume of AC has been recorded to be 2-fold in comparison to that of BC, although their distribution in between available micro pores and meso-macro pores has been documented to be almost similar. Owing to the reason the reason that the quantity of toluene adsorbed is directly not concerned with the surface area of the adsorbent or to the extent of distribution of the whole sum extent of porosity among micro pores and meso-macro pores, these outcomes satisfactorily revealed that greater target pollutant- adsorbent surface interactions must be encouraged [102]. **Table 6** refers to the utilization of biochar photo catalysts in removal of phenolic compounds from water bodies discharged from oil refineries, municipal waste treatment plant, coal conversion plants and spillage of oils.

5.2.4 Removal of Pharmaceutical pollutants

Biochar and biochar supported composites had been widely used for the elimination of pharmaceutical effluents from the wastewaters. TiO_2 incorporated reed straw derived biochar at 500°C for six hours as an adsorbent gave more satisfactory results for the elimination of Sulfamethoxazole than unmodified biochar, by photo catalytic degradation [103]. For the photo-catalytic mineralization of ciprofloxacin, the rice straw derived biochar functionalized with TiO_2 gave improved results because of role played by carbonyl group in the adsorption mechanism including electrostatic interaction, π-π interaction and H bond at pH range 5-9. The mineralization mechanism is concerned with the first defluorination reaction, and subsequently the mineralization of the piperazine ring [104]. Anthropogenic activities have increased the release of antipyretics, lifesaving drugs, antibiotics, analgesics, birth limiting pills and others in the water bodies. Since years, biochar has given satisfactory results as an adsorbent to eliminate pharmaceutical contaminants. In the present literature, deployment of biochars for the removal of sulfonamides, quinolones, tetracycline and other non-steroidal in addition to anti-inflammatory drugs (NSAID). Biochars derived from renewable sources demonstrated

100% recovery of pharmaceutical residues as water contaminants. Unlike commonly available adsorbents, biochar can be reused and reprocessed up to eighth folds with a negligible declined in the adsorptive remediation of water pollutants. The great recoveries of pharmaceutical contaminants deploying biochar derived from Eucommia ulmoides has been reported to be 1163 $mg.g^{-1}$ for tetracycline, 698.6 mg/g in case of norfloxacin by - biochar obtained from corncob, 596 $mg.g^{-1}$ in case of naproxen by derived from peanut shell, 400 $mg.g^{-1}$ for sulfamethoxazole with biochar originating from bagasse of sugarcane [105]. Compared with other carbonaceous materials, biochar is inexpensive and very commonly available, easy to deploy and having greater economic values, adsorptive elimination capacity and persulfate activation capability. In the previous research biochar has given satisfactory resulted in the elimination of drugs including, sulfamethoxazole (SMX), tetracycline (TC), levofloxacin (LEV), cephalexin (CPX) and acetaminophen (ACT), etc. through adsorptive elimination and persulfate-supported advanced oxidastion processes [106]. **Table 7** refers to the utilization of Biochar photo catalysts in elimination of pharmaceutical pollutants from waste water discharged from pharmaceuticals industries.

5.2.5 Other Potential applications

The conversion of biomass into biochar has been reported as an environmentally friendly, viable, and effective waste management strategy because it has the potential to simultaneously utilize biomass waste and protect the ecosystem from pollutants associated with agricultural practices. The selection of biochar for its application should be context-specific and based on a case-by-case assessment, taking into account the unique properties of the biochar and its intended functions. For instance the generation of hydrogen as carrier of energy, had been possible by photo-catalytic splitting of water. Clean and recyclable hydrogen can be produced, which later can be used as a potential fuel, by deploying renewable solar energy. The mechanism involved in the photo-catalytic production of hydrogen had been reported to consist of the following sequence of steps: First of all photo anode under goes oxidation by irradiation of light in order to generate electron–hole pairs. Then photo-generated holes carry out oxidation (loss of electrons) of water on the surface of photo-anode in order to generate molecular O_2 as well as H^+. Later, the transference of so photo produced electrons via an external route to the cathode and the reduction (gain of electrons) of H^+ by photo produced electrons on the surface of cathode for production of molecular H_2 [107]. After bringing the required modifications in the chemical profile of the soil such as total nitrogen, cation exchange capacity, available P_2O_5 saturation of base and pH of soil for the growth of maize supported by spread of fertilizers has been reported with increase in yield in the acidic soil [108]. Khushbu et al, has reported the improved growth of the plant in the biochar modified poor sandy soil because of the reduced stomatal resistance, better water retention capacity, leaf osmotic potential , and upgraded photosynthesis by boosting rate of electron transportation in II photosystem under both sufficiently watered and drought conditions [109]. Not only this but the research outcomes from Bhagyashree et al, had proved optimistic impacts of biochar on minimizing the diseases of plant including mildew and rust in wheat and numerous other pathogens also [110].

According to research conducted by Wael M et al, biomass yield and growth of Chenopodium quinoa and lettuce had been observed to be elevated up to many folds in a sandy-poor soil modified by 2% (w/w) with co-composted biochar although contrary to this, growth of maize plant was not influenced by deployment of flash-pyrolysis derived biochar at concentration of 45 t ha^{-1} for silty or sandy soil [111]. In the worlds of electrochemical gadgets, double layer capacitance, accounts for the electrostatic storage of charge by reversible ions adsorption on the surface of carbon without involvement of any electrochemical reaction. High exposed surface area of the composite is required in order to store greater amount of charge. The enormous exposed surface area because of greater porosity of biochar, low level of toxicity and low cost presents biochar as an efficient alternative to conventional carbonaceous materials in order to develop and upgrade electricity storage gadgets with relatively higher capacitance. Other than extent of porosity and surface area, the conductance of the tested biochar had been investigated optimistically with its double layer capacitance. It has also been observed that, in few cases, the improved wettability of the electrodes has resulted in improved double layered capacitance of the traditionally used carbonaceous material [112]. All above mentioned outcomes of the research conducted in the different areas are a testament of potential of the biochar, where these can further needs to be explored and investigated with diversified parameters.

5.3 Factors affecting photo-catalytic degradation

The rate of oxidation and efficacy of the photo-catalytic composite is highly determined by operational factors that decides the extent of the photo-degradation of the target pollutant. A lot of research has been conducted so far to publish the effect of these factors on the photo-catalytic performance and efficacy. Effect of these parametric factors has been discussed here and also has been illustrated in **Figure 10.**

(i) **Effect of reaction temperature:** Higher temperature of the photo-catalysis generally results in improved photo-catalytic performance. Generally, temperature between 20-80°C is the desired and required for effective photo degradation of the organic pollutant molecule [113]. The process temperature under 80°C supports the adsorption but subsequently decrease in temperature of reaction up to 0°C bring about an hike in realistic activation energy [114]. However temperature of reaction greater than >80°C favors the charge recombination rate and discourages the adsorptive elimination of organic contaminants on catalyst surface [115].

(ii) Effect of pollutant concentration: The photo-catalysis affected by the adsorptive elimination of textile pollutant molecule on surface of photo-catalyst. In photo-catalysis process, only the concentration of pollutant molecule adsorbed on the exposed photo-catalytic surface plays a significant role instead of the amount in matrix in bulk of the photo-catalyst. Adsorption of pollutant also governed by the initial pollutant concentration. It is noteworthy, that the percentage of degradation declines with greater pollutant concentration, by fixing the amount of photo-catalyst [116]. This present observation can be owing to the reason that as pollutant concentration if raised, more organic substances as contaminants get captured (adsorbed) on photo-catalyst surface but relatively smaller number of energetic photons are able to approach the photo-catalyst surface and consequently resulting in generation of lesser number of $^{\bullet}OH$, and hence in lower percentage of degradation [117].

(iii)Effect of pH: Undoubtedly, the Photo-degradation of pollutants is significantly impacted by pH of the experimental matrix. pH of the matrix alters the surface charge of photo-catalyst as well as alters catalytic reaction's potentials. Subsequently, the target pollutant molecule get adsorbed on surface is considerably altered ultimately bringing an alternation in the rate of reaction. Under alkaline or acidic conditions, the surface of Titania can be deprotonated or protonated respectively as per the reactions.

$TiOH + H^+ \rightarrow TiOH_2^+$ (Under acidic conditions)

$TiOH + OH^- \rightarrow TiO^- + H_2O$ (Under Alkaline conditions)

That is why surface of catalyst titania gets positively charged (cationic) under acidic conditions and anionic under alkaline (basic) situations. Titanium dioxide had been observed to exhibit relatively greater oxidizing performance at relatively lower pH, contrary to this, higher H^+ ions leads to reduced reaction rate. Dharmendra et al, has recorded the impact of pH on the performance of adsorption by biochar. In case pH of the practical situation is between 2.5 - 4.5, then potential of biochar to adsorb Cr^{3+} had been observed to be enhanced with the further increase in pH [118]. Besides, the adsorption amount of heavy metal anions gets reduced with rise in pH value.

(iv) **Effect of dopants on pollutant degradation**: Dopants, including transitional metals are generally incorporated to the photo catalyst to upgrades its response and to decrease the recombination of photo generated holes and electrons. Prime motive of doping with stuff stands for introduction of a bathochromic shift, with an intention to reduce the band gap or incorporation of states of intra-band gap, consequently resulting in absorption of more visible light. Although, heterogeneous photo-catalysis for organic dyes degradation using titanium dioxide (TiO_2) is quite promising technology with relatively poor efficiency of photo-quantum originating because of from the faster charge recombination rate of photo-generated holes and electrons. Besides this, owing to the wide band gap of TiO_2, it has been observed inactive under visible light (3.03eV - 3.18eV). This makes titania in-capable to deploy enormous potential solar energy in photo catalysis [119]. There are numerous techniques which allow TiO_2 to absorb photons of relatively low energy. Few of these techniques including modification of band gap by generating oxygen sub-stoichiometry and oxygen vacancies by non-metals such as co-doping of metal and non-metals surface modification through organic molecules and coupling of semi-conductor [120].

(v) **Effect of dissolved oxygen:** Dissolved molecular oxygen in the experimental matrix solution has been generally deployed as acceptor of electrons in photo catalytic interactions to affirm presence of sufficient electron scavengers to capture the excited electrons from conduction band by their re-combination. The oxygen had been observed to be incapable to impact adsorption on surface of catalyst. The rationale behind this is that reduction (gain of electrons) reaction takes place at a diversified sites from where oxidation takes places [121]. Dissolved oxygen is accountable for the cleavage of aromatic ring in organic contaminants present in aqueous environments. Dissolved oxygen leads to stabilization of radical intermediates, direct photo catalytic reactions and mineralization. The photo degradation of pollutant had been observed to be raised with higher dissolved oxygen. This is because of the formation of Oxygen free radical potentially can raise extent of the photo degradation [122].

(vi) Concentration and nature of pollutants: The rate of photo-catalytic degradation of target pollutant molecule is governed by the concentration, nature, composition, structure and other interfering impurities in aqueous media. Significant plethora of previously published literature has indicated the dependency of the rate of catalytic interactions on the amounts of pollutants in water. In water with high concentration of pollutants, the entire active sites on catalytic surface and hence declines the photonic efficiency and consequently leading to decreased performance efficacy of the photo-catalyst [123]. Not only the concentration of organic contaminants, but the chemical composition of the target pollutant also affects the efficiency of degradation performance of the photo-catalytic combination [124]. Organic moieties with electron withdrawing nature (nitrobenzene and benzoic acid) tightly get attached to the photo catalyst and that is why they are more prone to direct oxidation if compared with other electron donating groups. This is so because; the photo catalytic mineralization of aromatics contaminants had been reported to be greatly dependent on the nature of the substituent group. Additionally, if the nature of the target water pollutant is such that it binds to the photo catalyst surface, then whole s process will definitely be more efficient in elimination of such contaminants from the matrix.

(Vii) Effect of Inorganic ions: Wide variety of inorganic ions including copper, iron, zinc, magnesium, nitrate, bicarbonate, iron, sulphate, chloride and phosphate dissolved in waste water affects rate of photo-catalytic mineralization as these are in competition with the target contaminant for their adsorptive elimination on surface of catalyst. Photo-catalytic reduced performance efficiency has been documented if photo-catalyst has been utilized in fixed-bed configuration or slurry relating it to the strong restrictive effect from the presence of inorganic ions on the surface of the catalyst [125]. Numerous investigations had been carried out to determine the impact of inorganic cations and anions on photo-catalytic mineralization. Few cations of copper, iron, and anionic phosphate had been observed to decrease the photo-degradation efficacy in case these are available in little concentrations. However, cations including zinc, magnesium and calcium, had minute impact on the photo-degradation owing to the reason that cations with their optimum oxidation states are incapable to exert restrictive effect on the photo-mineralization process [126].

(vi) Impact of irradiation time and light intensity: Duration of irradiation and the light intensity both affects the pollutant degradation. It had been observed that at relatively lower light intensities of order of 0-20mWcm^{-2}, the rate of photo-mineralization had been observed to increases linearly with elevating light intensity (reaction is first order). Beside this, at intermediate light intensities (25mW/cm^{2}) the rate of reaction is dependent on the square root of the light intensity [127]. The independence of the reaction rate at high light intensities can be rationalized that, at low light intensity reactions involving formation of electron–hole is predominant and probability of recombination of electron–holes is negligible [128]. However, on raising the light intensity of light, the segregation of pair of electron–hole had been observed to compete with re-combination, which gradually reduces its impact on the rate of reaction [129].

(vii) Effect of size and structure of the photo-catalyst: The morphological features of the catalytic exposed surface including particle size and extent of agglomeration are the crucial factors in photo-catalytic degradation owing to their direct relationship between organic pollutant and the occupancy of the quantity of active site on surface of photo-catalyst. Quantity of photon striking the surface of photo-catalyst also affects the reaction's rate because the reaction occurs only among the adsorbed pollutants molecules on the photo-catalyst [130].

5.4 Stability and Recyclability:

Many reports are available by different researchers groups highlighting the recyclable nature of composites of biochar. Investigations pertaining to recycability had been performed deploying one-step and two step Bi-TNT composites to investigate the stability of photo-catalysts. Recycle evaluation testing parameters were the identical as those for the photo-mineralization of the industrial waste water [131]. The optimized operational parameters for Bi-TNT two-step and one-step catalysts were utilized for the recycling evaluations. The Bi-TNT photo-catalytic composite was reutilized for about consecutive five cycles. The photo-catalytic degradation efficiency by one-step and two-step Bi-TNT composites for methylene blue dye has decreased 4% and 14%, respectively. Total organic carbon (TOC) elimination in the industrial effluent by one -step and two-step Bi-TNT composites has reduced 16% and 5%, respectively. Composite fabricated by one-step was reported to be more durable and stable for consecutive five cycles, because of the Bi coupling and nanotube formation taking place simultaneously [132]. It was observed that the mineralization of MB and DCHCl by Bi_5O_7I/TWB/PCN (40 wt%) deploying a halogen lamp up to 88%, and 86.2% respectively, about four cycles, expressing its reasonable recyclability [133]. However, more investigations with numerous photoactive materials are required to be conducted with an objective of extension of knowledge and emphasize more on the pollutant efficacies in practical-time water treatments, continuous reuse of the deployed catalyst with sunlight under ordinary conditions. The utilization of HPLC with diversified detectors deploying either MS or combination of GC–MS for surface charge of composites for mechanistic mineralization investigations in the presence of the contaminated water conditions are required to assure the potential of the immobilized photo catalytic substrate [134].

The structure of biochar depends upon the arrangement of carbon atoms constituting either an amorphous phase or a crystalline phase. The assessment of stability of biochar can be performed by evaluation the carbon present in stable structure of biochar. The structure of carbon had been deployed since years for determining the element in investigating stability of biochar. Aromaticity and aromatic condensation are the prime indicators indicating the carbon structure of biochar. Biochar rich in high extent of aromaticity and aromatic condensation are highly stable against biological and thermo-chemical degradation [135]. The bond between carbon and carbon and aromatic character is exhibit the elemental composition of the biochar. The stability of biochar characteristic features depends upon pH, pore structure; adsorption mechanism, minerals, particle size and surface area of the biochar [41]. The direct and more reliable stability results are obtained if biochar is evaluated either by modeling or incubation methods. Under incubation conditions, longevity results are given by this method. Modeling of data are the factors governing the stability. For assessment of time required for the complete degradation of biochar for the sake of biochar stability is assessed by biochar incubation [85]. Longevity calculation is not possible because complete degradation of biochar takes hundreds of years. However, modeling process and incubation is not cost effectives and consumes a lot of time [136]. The designing of novel approach for investigating stability of biochar shall increase the applicability of biochar for mitigation of changes in climate. The structural damage of biochar is also one of the reasons of biochar instability [87]. If biochar is used for the treatment of environment it can prove as a potential robust material for converting waste bio mass into valuable commodity because biochar had been documented to possess several merits including cost effective, recyclability and variety of different types of raw materials [137].

6. Challenges and prospects for future

Each material can exhibit both beneficial properties and inherent limitations. To achieve optimal results, it is essential to first identify these limitations and then focus research efforts on overcoming them. In the case of biochar, these limitations include selecting an appropriate feedstock material and determining the optimal thermal treatment conditions. Properties such as surface morphology—including pore structure, pore diameter, surface functionalities, and surface area—are heavily dependent on the nature of the feedstock. Biochar derived from different feed stock's may show varying efficacy in treating different contaminants. Therefore, selecting a suitable biochar for specific targets can pose significant challenges for large-scale and real-world applications. Additionally, surface activation may be required, which is often expensive, non-recyclable, and may lead to equipment corrosion, complicating reusability. Besides these issues, several other aspects require further research, including poor mechanical strength and low electrical conductivity.

Photo-corrosion and leaching of biochar-supported catalysts remain unresolved issues. Environmental changes can cause the catalyst to detach from biochar, affecting stability. Overcoming these challenges is crucial for industrial application. Pilot-scale studies are needed to address these issues and enhance large-scale wastewater treatment. The challenge is scaling for industrial water treatment, requiring economical technology upgrades. The laboratory studies focus on temperature and pH while industrial factors like flow rate and pressure significantly impact the photo-catalytic process and catalyst stability, thus the research also need to be explored in such direction. However, the biochar supported photo catalyst composite had the outstanding features to treat recalcitrant organic pollutant from effluent; the photo-catalysis based research is at the laboratory scale demanding substantial efforts for its deployment on industrial level for the treatment of larger volume of the effluent. In order to apply the results of photo-catalytic degradation on the industrial scale, emphasize is to be given to the following points:

1) Large scale availability of the bio mass throughout the year, for the production of biochar owing to the enormous volume of the industrial wastewater
2) The investigation should not only be restricted to the agricultural waste but should be carried out on the industrial scale of waste water including municipal sludge and production factories based solid waste
3) In-depth elaborated research has to be carried out in order to functionalize the biochar supported composite to be efficient as well as effective in complex pollutants waste water interfering in the photo-catalytic performance.
4) The construction and the design of bio-reactor of required infrastructure and dimensions should be appropriate to apply and re-utilize these photo-catalytic composites for industrial scale treatment of effluent installations.

The present review highlighted the widely available bio mass deployed for the synthesis of biochar and their utilization in diversified areas. The biochar functionalization techniques, various biochar supported photo catalyst composite deployed for photo catalytic mineralization of organic pollutants including pharmaceutical product, textile dyes, and phenolic compounds as well as the challenges dealing in the real-time practical deployment of these photo catalytic composite for industrial based wastewater treatment processes.

Ethical approval statement

This declaration is “not applicable”.

Funding statement

N/A.

Informed consent

All authors and co-authors have given their consent for publication of the research work to this journal.

CRediT authorship contribution statement

Conceptualization, methodology, supervision: **Ajay Kumar**. Writing—original draft: **Pooja Dhiman.** Formal Analysis & Data curation: **Manisha Dhiman**, **Manita Thakur, Sourav Gautam**. Visualization, writing—review and editing: **Arush Sharma.**

Declaration of Competing Interest

The authors declare that they have no known competing financial interests or personal relationships that could have appeared to influence the work reported in this paper.

Data availability

Data will be made available on request.

Acknowledgment

Not applicable

References

[1] M. Hawryluk-Sidoruk, M. Raczkiewicz, P. Krasucka, W. Duan, O. Mašek, R. Zarzycki, R. Kobyłecki, B. Pan, P. Oleszczuk, Effect of biochar chemical modification (acid, base and hydrogen peroxide) on contaminants content depending on feedstock and pyrolysis conditions, Chem. Eng. J. 481 (2024) 148329.

[2] G.L. Tihin, K.H. Mo, J.C. Juan, H.C. Ong, N. Asikin-Mijan, H.V. Lee, Enhanced energy recovery of non-hazardous organic wastes via moderate pyrolysis with natural calcium-and potassium-based additives, J. Therm. Anal. Calorim. (2024) 1–15.

[3] K. Kaur, R. Kaur, H. Kaur, A systematic review of lignocellulosic biomass for remediation of environmental pollutants, Appl. Surf. Sci. Adv. 19 (2024) 100547.

[4] Y. Jiang, C. Ming, K. Sun, L. Zhang, S. Zhang, Z. Cui, D. Wang, C. Leng, X. Hu, Enhanced abundance of oxygen-containing intermediates from pre-oxidation of poplar sawdust facilitates generation of porous structures in activation with phosphoric acid, Sustain. Mater. Technol. 39 (2024) e00815.

[5] S. Bhowmick, R. Mitra, R. Kumar, S. Yadav, S. Tripathi, S. Mukherjee, R. Sen, An Insight into the Recent Developments of Biofuel Production from Microalgae, Biofuels (2024) 311–334.

[6] A.A. Najim, A.Y. Radeef, I. al-Doori, Z.H. Jabbar, Immobilization: the promising technique to protect and increase the efficiency of microorganisms to remove contaminants, J. Chem. Technol. Biotechnol. (2024).

[7] S. Bhattacharya, S.A. Hossain, A. Bhowal, P. Das, Integral approach of adsorption and photo-degradation of Bisphenol A using pyrolyzed rice straw biochar coated with metal oxide: batch, mechanism and optimization, Sādhanā 49 (2024) 1–16.

[8] M. Abou Rjeily, M. Chaghouri, C. Gennequin, E. Abi Aad, J.H. Randrianalisoa, Investigating co-production of syngas, biochar, and bio-oil from flax shives biomass by pyrolysis and in-line catalytic hybrid reforming, Biomass Convers. Biorefinery (2023) 1–27.

[9] A. Kumar, T.S. Dabodiya, D. Ramamoorthy, Biochar-Based Nanocomposites, Biochar-Based Nanocomposites Contam. Manag. Synth. Contam. Removal, Environ. Sustain. (2023) 85.

[10] N. Abdullah, R.M. Taib, N.S.M. Aziz, M.R. Omar, N.M. Disa, Banana pseudo-stem biochar derived from slow and fast pyrolysis process, Heliyon 9 (2023).

[11] I.E. Rushimisha, X. Li, T. Han, X. Chen, A.S.I. Abdoul Magid, Y. Sun, Y. Li, Application of biochar on soil bioelectrochemical remediation: behind roles, progress, and potential, Crit. Rev. Biotechnol. 44 (2024) 120–138.

[12] T. Sharma, I.G. Hakeem, A.B. Gupta, J. Joshi, K. Shah, A.K. Vuppaladadiyam, A. Sharma, Parametric influence of process conditions on thermochemical techniques for biochar production: A state-of-the-art review, J. Energy Inst. (2024) 101559.

[13] D. KP, Biochars and Their Application as Transesterification Catalyst: A Review, (2023).

[14] M. Gholizadeh, S. Meca, S. Zhang, F. Clarens, X. Hu, Understanding the dependence of biochar properties on different types of biomass, Waste Manag. 182 (2024) 142–163.

[15] Y. Niu, S. Han, Y. Hu, M. Yang, F. Han, Non-isothermal and isothermal co-pyrolysis characteristics of coal gangue/coal slime and pine sawdust: Thermogravimetric analyzer and fixed bed pyrolysis reactor study, Int. J. Hydrogen Energy 59 (2024) 1230–1243.

[16] M. Yaseen, M.A.K. Khattak, M. Humayun, M. Usman, S.S. Shah, S. Bibi, B.S.U.

Hasnain, S.M. Ahmad, A. Khan, N. Shah, A Review of Supercapacitors: Materials Design, Modification, and Applications. Energies 2021, 14, 7779, (2021).

[17] M. Mashuni, M. Jahiding, L.O. Kadidae, N.A. Yanti, F.H. Hamid, Chromatography and spectroscopy analysis of the pyrolysis products of coconut shell as a strong antifungal agent on cocoa seeds, in: AIP Conf. Proc., AIP Publishing, 2024.

[18] E.C. Emenike, K.O. Iwuozor, J.O. Ighalo, J.O. Bamigbola, E.O. Omonayin, H.T. Ojo, J. Adeleke, A.G. Adeniyi, Advancing the circular economy through the thermochemical conversion of waste to biochar: a review on sawdust waste-derived fuel, Biofuels 15 (2024) 433–447.

[19] X.-F. Tan, S.-S. Zhu, R.-P. Wang, Y.-D. Chen, P.-L. Show, F.-F. Zhang, S.-H. Ho, Role of biochar surface characteristics in the adsorption of aromatic compounds: Pore structure and functional groups, Chinese Chem. Lett. 32 (2021) 2939–2946.

[20] Y. Wang, S. Lin, L. Liu, F. Wang, X. Yang, G. Qiu, High-efficiency electrochemical removal of Cd (II) from wastewater using birnessite-biochar composites: performance and mechanism, Environ. Monit. Assess. 195 (2023) 549.

[21] A. Al-Rumaihi, M. Shahbaz, G. Mckay, H. Mackey, T. Al-Ansari, A review of pyrolysis technologies and feedstock: A blending approach for plastic and biomass towards optimum biochar yield, Renew. Sustain. Energy Rev. 167 (2022) 112715.

[22] F. Amalina, A.S. Abd Razak, S. Krishnan, H. Sulaiman, A.W. Zularisam, M. Nasrullah, Advanced techniques in the production of biochar from lignocellulosic biomass and environmental applications, Clean. Mater. 6 (2022) 100137.

[23] Z. Mo, C. Li, Y. Zhang, J. Ren, Z. Zhu, J. Liang, M. Ye, Z. Zhu, S. Zhu, W. Yang, Ball-milled pyrite@ biochar induced percarbonate activation for sustainable degradation of antibiotic norfloxacin at inherent pH environment, Sep. Purif. Technol. 335 (2024) 126202.

[24] Y. Huang, D. Zhang, H. Cheng, Y. He, G. Hu, Effective removal and recovery of phosphorus using ZnAl-COOH-modified biochar via hydrogen bonds, Sep. Purif. Technol. 329 (2024) 125159.

[25] L. Liang, F. Xi, W. Tan, X. Meng, B. Hu, X. Wang, Review of organic and inorganic pollutants removal by biochar and biochar-based composites, Biochar 3 (2021) 255–281.

[26] H. Li, X. Dong, E.B. da Silva, L.M. de Oliveira, Y. Chen, L.Q. Ma, Mechanisms of metal sorption by biochars: Biochar characteristics and modifications, Chemosphere 178 (2017) 466–478.

[27] X. He, H. Yin, L. Han, R. Cui, C. Fang, G. Huang, Effects of biochar size and type on gaseous emissions during pig manure/wheat straw aerobic composting: Insights into multivariate-microscale characterization and microbial mechanism, Bioresour. Technol. 271 (2019) 375–382.

[28] D.R. Vaghela, A. Pawar, N.L. Panwar, D. Sharma, Modelling and optimization of biochar-based adsorbent derived from wheat straw using response surface methodology on adsorption of Pb2+, Int. J. Environ. Res. 17 (2023) 9.

[29] R. Li, Y. Wu, X. Lou, H. Li, J. Cheng, B. Shen, L. Qin, Porous biochar materials for sustainable water treatment: synthesis, modification, and application, Water 15 (2023) 395.

[30] Z. Zhang, G. Huang, P. Zhang, J. Shen, S. Wang, Y. Li, Development of iron-based biochar for enhancing nitrate adsorption: Effects of specific surface area, electrostatic force, and functional groups, Sci. Total Environ. 856 (2023) 159037.

[31] Y. Liang, Y. Wang, N. Ding, L. Liang, S. Zhao, D. Yin, Y. Cheng, C. Wang, L. Wang, Preparation and hydrogen storage performance of poplar sawdust biochar with high specific surface area, Ind. Crops Prod. 200 (2023) 116788.

[32] J. Fan, F. Li, D. Fang, Q. Chen, Q. Chen, H. Wang, B. Pan, Effects of hydrophobic coating on properties of hydrochar produced at different temperatures: Specific surface area and oxygen-containing functional groups, Bioresour. Technol. 363 (2022) 127971.

[33] C. Wen, T. Liu, D. Wang, Y. Wang, H. Chen, G. Luo, Z. Zhou, C. Li, M. Xu, Biochar as the effective adsorbent to combustion gaseous pollutants: preparation, activation, functionalization and the adsorption mechanisms, Prog. Energy Combust. Sci. 99 (2023) 101098.

[34] P.R. Rout, D.S. Pandey, M. Haynes-Parry, C. Briggs, H.L.C. Manuel, R. Umapathi, S. Mukherjee, S. Panigrahi, M. Goel, Sustainable valorisation of animal manures via thermochemical conversion technologies: an inclusive review on recent trends, Waste and Biomass Valorization 14 (2023) 553–582.

[35] A. Halim, N. Sa'adah, J. Vijayanathan, R. Abdullah, J.S. Yaacob, M.A. Mazlan, R. Ahmad, P. Elham, A.S. Kassim, Influence of different pyrolysis temperature on the characteristics of forestry waste biochar for sodium adsorption, J. Mater. Cycles Waste Manag. 26 (2024) 894–907.

[36] C. Zhang, Z. Zhang, L. Zhang, Q. Li, C. Li, G. Chen, S. Zhang, Q. Liu, X. Hu, Evolution of the functionalities and structures of biochar in pyrolysis of poplar in a

wide temperature range, Bioresour. Technol. 304 (2020) 123002.

[37] F. Zhu, Z. Wang, J. Huang, W. Hu, D. Xie, Y. Qiao, Efficient adsorption of ammonia on activated carbon from hydrochar of pomelo peel at room temperature: Role of chemical components in feedstock, J. Clean. Prod. 406 (2023) 137076.

[38] X. Li, Z. Huang, S. Shao, Y. Cai, Machine learning prediction of physical properties and nitrogen content of porous carbon from agricultural wastes: Effects of activation and doping process, Fuel 356 (2024) 129623.

[39] J. Li, C. Peng, J. Li, J. Wang, H. Zhang, Insight into sodium storage behaviors in hard carbon by reaxff molecular dynamics simulation, Energy & Fuels 36 (2022) 5937–5952.

[40] R.K. Sharma, T.P. Singh, S. Mandal, D. Azad, S. Kumar, Chemical treatments for biochar modification: opportunities, limitations and advantages, in: Eng. Biochar Fundam. Prep. Charact. Appl., Springer, 2022: pp. 65–84.

[41] L. Leng, Q. Xiong, L. Yang, H. Li, Y. Zhou, W. Zhang, S. Jiang, H. Li, H. Huang, An overview on engineering the surface area and porosity of biochar, Sci. Total Environ. 763 (2021) 144204.

[42] B. Qiu, X. Tao, H. Wang, W. Li, X. Ding, H. Chu, Biochar as a low-cost adsorbent for aqueous heavy metal removal: A review, J. Anal. Appl. Pyrolysis 155 (2021) 105081.

[43] R. Shan, Y. Shi, J. Gu, J. Bi, H. Yuan, B. Luo, Y. Chen, Aqueous Cr (VI) removal by biochar derived from waste mangosteen shells: Role of pyrolysis and modification on its absorption process, J. Environ. Chem. Eng. 8 (2020) 103885.

[44] X. Li, C. Wang, J. Zhang, J. Liu, B. Liu, G. Chen, Preparation and application of magnetic biochar in water treatment: A critical review, Sci. Total Environ. 711 (2020) 134847.

[45] G. Yin, X. Chen, B. Sarkar, N.S. Bolan, T. Wei, H. Zhou, H. Wang, Co-adsorption mechanisms of Cd (II) and As (III) by an Fe-Mn binary oxide biochar in aqueous solution, Chem. Eng. J. 466 (2023) 143199.

[46] Y. Wang, T. Jiang, X. Fan, H. Zou, J. Zhao, Degradation of Acid Orange II by sludge-derived biochar supported Cu/Fe bimetallic particles activating persulfate, Desalin. WATER Treat. 256 (2022) 314–327.

[47] J. Dobrzyńska, A. Wysokińska, R. Olchowski, Raspberry stalks-derived biochar, magnetic biochar and urea modified magnetic biochar-Synthesis, characterization and application for As (V) and Cr (VI) removal from river water, J. Environ. Manage. 316 (2022) 115260.

[48] R. Jain, Recent advances of magnetite nanomaterials to remove arsenic from water, RSC Adv. 12 (2022) 32197–32209.

[49] Faheem, J. Du, S.H. Kim, M.A. Hassan, S. Irshad, J. Bao, Application of biochar in advanced oxidation processes: supportive, adsorptive, and catalytic role, Environ. Sci. Pollut. Res. 27 (2020) 37286–37312.

[50] M. Zahedifar, N. Seyedi, S. Shafiei, M. Basij, Surface-modified magnetic biochar: highly efficient adsorbents for removal of Pb (II) and Cd (II), Mater. Chem. Phys. 271 (2021) 124860.

[51] P. Pillai, S. Dharaskar, Arsenic Removal Using Nanoparticles from Groundwater: A Review, Handb. Solid Waste Manag. Sustain. through Circ. Econ. (2020) 1–15.

[52] P. Wu, P. Cui, Y. Zhang, M.E. Alves, C. Liu, D. Zhou, Y. Wang, Unraveling the molecular mechanisms of Cd sorption onto MnOx-loaded biochar produced from the Mn-hyperaccumulator Phytolacca americana, J. Hazard. Mater. 423 (2022) 127157.

[53] X. Qi, H. Yin, M. Zhu, X. Yu, P. Shao, Z. Dang, MgO-loaded nitrogen and phosphorus self-doped biochar: High-efficient adsorption of aquatic Cu2+, Cd2+, and Pb2+ and its remediation efficiency on heavy metal contaminated soil, Chemosphere 294 (2022) 133733.

[54] J. Lu, Y. Qiu, L. Zhang, J. Wang, C. Li, P. Wang, L. Ren, Effects of Fe3O4 NMs based Fenton-like reactions on biodegradable plastic bags in compost: new insight into plastisphere community succession, co-composting efficiency and free radical in situ aging theory, J. Hazard. Mater. (2024) 133689.

[55] F. Vargas, E. Lucena-Mendoza, T. Zoltan, Y. Torres, M. León, B. Angulo, G.I. Tovar, Photochemical and Sonochemical Strategies in Advanced Oxidation Processes for Micropollutants' Treatments, in: Adv. Oxid. Process. Micropollutant Remediat., CRC Press, 2024: pp. 65–98.

[56] F. Yang, J. Li, H. Wang, Z. Li, Z. Wang, Metal organic framework-assisted sonodynamic oxidation platform for removing organic contaminants in water, J. Clean. Prod. (2024) 142155.

[57] J.-R. Zheng, C.-S. Yuan, Comparing the Photocatalytic Oxidation Efficiencies of Elemental Mercury Using Metal-Oxide-Modified Titanium Dioxide under the Irradiation of Ultra-Violet Light, Catalysts 14 (2024) 209.

[58] M.T. Samadi, A. Rezaie, A.A. Ebrahimi, A. Hossein Panahi, K. Kargarian, H. Abdipour, The utility of ultraviolet beam in advanced oxidation-reduction processes: a review on the mechanism of processes and possible production free radicals, Environ.

Sci. Pollut. Res. 31 (2024) 6628–6648.

[59] R. Luque, A. Ahmad, S. Tariq, M. Mubashir, M.S. Javed, S. Rajendran, R.S. Varma, A. Ali, C. Xia, Functionalized interconnected porous materials for heterogeneous catalysis, energy conversion and storage applications: Recent advances and future perspectives, Mater. Today (2023).

[60] A. Mei, Z. Xu, X. Wang, Y. Liu, J. Chen, J. Fan, Q. Shi, Photocatalytic materials modified with carbon quantum dots for the degradation of organic pollutants under visible light: A review, Environ. Res. 214 (2022) 114160.

[61] Y. Tan, Y. Duan, Q. Chi, R. Wang, Y. Yin, D. Cui, S. Li, A. Wang, R. Ma, B. Li, The role of reactive oxygen species in plant response to radiation, Int. J. Mol. Sci. 24 (2023) 3346.

[62] C.M. Curieses Andrés, J.M. Pérez de Lastra, C. Andrés Juan, F.J. Plou Gasca, E. Pérez-Lebeña, Superoxide Anion Chemistry—Its Role at the Core of the Innate Immunity, (2023).

[63] D. Ayodhya, Semiconductors-based Z-scheme materials for photoelectrochemical water splitting: A review, Electrochim. Acta 448 (2023) 142118.

[64] S. Lee, H.-S. Bae, W. Choi, Selective control and characteristics of water oxidation and dioxygen reduction in environmental photo (electro) catalytic systems, Acc. Chem. Res. 56 (2023) 867–877.

[65] H. Qin, K. Sun, P. Hao, H. Yuan, Y. Shen, A. Bian, Y. Cui, J. Hou, W. Shi, C. Li, Efficient photocatalytic H2O2 production by using unstable SO functional groups as oxygen adsorption and active sites in shuttlecock waste-derived N, S-doped carbon dots, J. Catal. 435 (2024) 115579.

[66] W. Shi, C. Shi, W. Sun, Y. Liu, F. Guo, X. Lin, Dual enhancement of photooxidation and photoreduction activity by coating CdS nanoparticles on lignin-based biomass carbon with irregular flower-like structure, J. Mater. Sci. 56 (2021) 19452–19465.

[67] F. Guo, C. Shi, W. Sun, Y. Liu, X. Lin, W. Shi, Pomelo biochar as an electron acceptor to modify graphitic carbon nitride for boosting visible-light-driven photocatalytic degradation of tetracycline, Chinese J. Chem. Eng. 48 (2022) 1–11.

[68] J. Qu, Y. Wang, X. Tian, Z. Jiang, F. Deng, Y. Tao, Q. Jiang, L. Wang, Y. Zhang, KOH-activated porous biochar with high specific surface area for adsorptive removal of chromium (VI) and naphthalene from water: Affecting factors, mechanisms and reusability exploration, J. Hazard. Mater. 401 (2021) 123292.

[69] N. Karić, A.S. Maia, A. Teodorović, N. Atanasova, G. Langergraber, G. Crini, A.R.L.

Ribeiro, M. Đolić, Bio-waste valorisation: Agricultural wastes as biosorbents for removal of (in) organic pollutants in wastewater treatment, Chem. Eng. J. Adv. 9 (2022) 100239.

[70] K. Chen, J. Jiang, C. Huang, L. Wang, X. Wang, Investigating the potential of mineral precipitation in co-pyrolysis biochar: Development of a novel Cd (II) adsorption material utilizing dual solid waste, Bioresour. Technol. (2024) 130762.

[71] Y. Xie, G. Zhou, X. Huang, X. Cao, A. Ye, Y. Deng, J. Zhang, C. Lin, R. Zhang, Study on the physicochemical properties changes of field aging biochar and its effects on the immobilization mechanism for Cd2+ and Pb2+, Ecotoxicol. Environ. Saf. 230 (2022) 113107.

[72] Y. Deng, S. Huang, D.A. Laird, X. Wang, Z. Meng, Adsorption behaviour and mechanisms of cadmium and nickel on rice straw biochars in single-and binary-metal systems, Chemosphere 218 (2019) 308–318.

[73] P. Bhat, N. Jain, N. Naik, A. V Samrot, S.A. Salmataj, Adsorptive removal of chromium from simulated industrial wastewater using jungle geranium-derived biosorbents, ES Mater. Manuf. 22 (2023) 1070.

[74] S. Bose, P.S. Kumar, G. Rangasamy, G. Prasannamedha, S. Kanmani, A review on the applicability of adsorption techniques for remediation of recalcitrant pesticides, Chemosphere 313 (2023) 137481.

[75] A. Mandal, A. Kumar, N. Singh, Sorption mechanisms of pesticides removal from effluent matrix using biochar: Conclusions from molecular modelling studies validated by single-, binary and ternary solute experiments, J. Environ. Manage. 295 (2021) 113104.

[76] D. Losacco, C. Campanale, M. Triozzi, C. Massarelli, V.F. Uricchio, Application of Wood and Vegetable Waste-Based Biochars in Sustainable Agriculture: Evaluation on Nitrate Leaching, Pesticide Fate, Soil Properties, and Brassica oleracea Growth, Environments 11 (2024) 13.

[77] H. Li, S. Liu, S. Qiu, L. Sun, X. Yuan, D. Xia, Catalytic ozonation oxidation of ketoprofen by peanut shell-based biochar: effects of the pyrolysis temperatures, Environ. Technol. 43 (2022) 848–860.

[78] N.A. Baharum, H.M. Nasir, M.Y. Ishak, N.M. Isa, M.A. Hassan, A.Z. Aris, Highly efficient removal of diazinon pesticide from aqueous solutions by using coconut shell-modified biochar, Arab. J. Chem. 13 (2020) 6106–6121.

[79] A.K. Rana, Y.K. Mishra, V.K. Gupta, V.K. Thakur, Sustainable materials in the

removal of pesticides from contaminated water: Perspective on macro to nanoscale cellulose, Sci. Total Environ. 797 (2021) 149129.

[80] A. Nayak, P. Chaudhary, B. Bhushan, K. Ghai, S. Singh, M. Sillanpää, Removal of emergent pollutants: A review on recent updates and future perspectives on polysaccharide-based composites vis-à-vis traditional adsorbents, Int. J. Biol. Macromol. (2024) 129092.

[81] A.K. Patel, R.R. Singhania, A. Pal, C.-W. Chen, A. Pandey, C.-D. Dong, Advances on tailored biochar for bioremediation of antibiotics, pesticides and polycyclic aromatic hydrocarbon pollutants from aqueous and solid phases, Sci. Total Environ. 817 (2022) 153054.

[82] A. Srikhaow, W. Chaengsawang, T. Kiatsiriroat, P. Kajitvichyanukul, S.M. Smith, Adsorption kinetics of imidacloprid, acetamiprid and methomyl pesticides in aqueous solution onto eucalyptus woodchip derived biochar, Minerals 12 (2022) 528.

[83] D. Wang, R.A. Root, J. Chorover, Biochar-templated surface precipitation and inner-sphere complexation effectively removes arsenic from acid mine drainage, Environ. Sci. Pollut. Res. 28 (2021) 45519–45533.

[84] P. Samanta, S. Dey, J. Jung, A.R. Ghosh, Mechanism of metal sorption by biochar, BioChar Appl. Bioremediation Contam. Syst. (2022) 117.

[85] M. Arif, T. Jan, M. Riaz, S. Fahad, M. Adnan, Amanullah, K. Ali, I.A. Mian, B. Khan, F. Rasul, Biochar; a remedy for climate change, Environ. Clim. Plant Veg. Growth (2020) 151–171.

[86] Y. Huang, Y. Huang, L. Fang, B. Zhao, Y. Zhang, Y. Zhu, Z. Wang, Q. Wang, F. Li, Interfacial chemistry of mercury on thiol-modified biochar and its implication for adsorbent engineering, Chem. Eng. J. 454 (2023) 140310.

[87] L. Xiang, S. Liu, S. Ye, H. Yang, B. Song, F. Qin, M. Shen, C. Tan, G. Zeng, X. Tan, Potential hazards of biochar: The negative environmental impacts of biochar applications, J. Hazard. Mater. 420 (2021) 126611.

[88] G. Manickavasagam, C. He, K.-Y.A. Lin, M. Saaid, W.-D. Oh, Recent advances in catalyst design, performance, and challenges of metal-heteroatom-co-doped biochar as peroxymonosulfate activator for environmental remediation, Environ. Res. (2024) 118919.

[89] X. Zhou, Y. Zhu, Q. Niu, G. Zeng, C. Lai, S. Liu, D. Huang, L. Qin, X. Liu, B. Li, New notion of biochar: A review on the mechanism of biochar applications in advannced oxidation processes, Chem. Eng. J. 416 (2021) 129027.

[90] Q. Jin, J. Kang, Q. Chen, J. Shen, F. Guo, Z. Chen, Efficiently enhanced Fenton-like reaction via Fe complex immobilized on silica particles for catalytic hydrogen peroxide degradation of 2, 4-dichlorophenol, Appl. Catal. B Environ. 268 (2020) 118453.

[91] M. Bhattu, J. Singh, Recent advances in nanomaterials based sustainable approaches for mitigation of emerging organic pollutants, Chemosphere 321 (2023) 138072.

[92] S.A. Bradford, C. Shen, H. Kim, R.J. Letcher, J. Rinklebe, Y.S. Ok, L. Ma, Environmental applications and risks of nanomaterials: An introduction to CREST publications during 2018–2021, Crit. Rev. Environ. Sci. Technol. 52 (2022) 3753–3762.

[93] J. Ma, G. Ankit, F. Zhong, C. Li, N. Liu, W. Niu, H. Cao, Coupling behavior and enhancement mechanism of porous structure, graphite microcrystals, and oxygen-containing groups of activated biochar for the adsorption of phenol, Environ. Sci. Water Res. Technol. 9 (2023) 1944–1957.

[94] R. Suresh, S. Rajendran, L.C. Ponce, Waste-based adsorbents for the removal of emerging pollutants and their adsorption mechanisms, in: Sustain. Technol. Remediat. Emerg. Pollut. from Aqueous Environ., Elsevier, 2024: pp. 203–221.

[95] S. Kang, J. Jung, J.K. Choe, Y.S. Ok, Y. Choi, Effect of biochar particle size on hydrophobic organic compound sorption kinetics: applicability of using representative size, Sci. Total Environ. 619 (2018) 410–418.

[96] M. Zhu, Y. Liu, J. Xu, Y. He, Compound-specific stable isotope analysis for characterization of the transformation of γ-HCH induced by biochar, Chemosphere 314 (2023) 137729.

[97] M. Chen, Z. Yan, J. Luan, X. Sun, W. Liu, X. Ke, π-π electron-donor-acceptor (EDA) interaction enhancing adsorption of tetracycline on 3D PPY/CMC aerogels, Chem. Eng. J. 454 (2023) 140300.

[98] Y. Hou, G. Huang, J. Li, Q. Yang, S. Huang, J. Cai, Hydrothermal conversion of bamboo shoot shell to biochar: Preliminary studies of adsorption equilibrium and kinetics for rhodamine B removal, J. Anal. Appl. Pyrolysis 143 (2019) 104694.

[99] S. Ekman, G.S. Dos Reis, E. Laisné, J. Thivet, A. Grimm, E.C. Lima, M. Naushad, G.L. Dotto, Synthesis, characterization, and adsorption properties of nitrogen-doped nanoporous biochar: efficient removal of reactive Orange 16 Dye and colorful effluents, Nanomaterials 13 (2023) 2045.

[100] M.A. El-Nemr, N.M. Abdelmonem, I.M.A. Ismail, S. Ragab, A. El Nemr, The

efficient removal of the hazardous Azo Dye Acid Orange 7 from water using modified biochar from Pea peels, Desalin. Water Treat 203 (2020) 327–355.

[101] X. Sun, H. Fu, M. Bao, W. Liu, C. Luo, Y. Li, Y. Li, J. Lu, Development of a new hydrophobic magnetic biochar for removing oil spills on the water surface, Biochar 4 (2022) 60.

[102] M. Luo, L. Wang, H. Li, Y. Bu, Y. Zhao, J. Cai, Hierarchical porous biochar from kelp: Insight into self-template effect and highly efficient removal of methylene blue from water, Bioresour. Technol. 372 (2023) 128676.

[103] S. Minaei, K.Z. Benis, K.N. McPhedran, J. Soltan, Adsorption of sulfamethoxazole and lincomycin from single and binary aqueous systems using acid-modified biochar from activated sludge biomass, J. Environ. Manage. 358 (2024) 120742.

[104] Z. Li, D. Dong, L. Zhang, Y. Li, Z. Guo, Effect of fulvic acid concentration levels on the cleavage of piperazinyl and defluorination of ciprofloxacin photodegradation in ice, Environ. Pollut. 307 (2022) 119499.

[105] S.W. Sherpa, M. Ponnuchamy, A. Kapoor, M.M. Jacob, P. Sivaraman, Facile removal of sulfamethoxazole antibiotic from contaminated water using bagasse-derived pyrolytic biocarbon: Parametric assessment, mechanistic insights and scale-up analysis, J. Water Process Eng. 60 (2024) 105110.

[106] Z. Kang, X. Jia, Y. Zhang, X. Kang, M. Ge, D. Liu, C. Wang, Z. He, A review on application of biochar in the removal of pharmaceutical pollutants through adsorption and persulfate-based AOPs, Sustainability 14 (2022) 10128.

[107] S. Shen, S. Wang, Water Photo-and Electro-Catalysis: Mechanisms, Materials, Devices, and Systems, John Wiley & Sons, 2024.

[108] M. Dejene, Opportunities to Alleviate Soil Acidity Impact Through Exploitation of Diverse Liming Materials Integrated with Different Phosphatic Fertilizer Sources in Ethiopia, (2021).

[109] K. Kumari, R. Kumar, N. Bordoloi, T. Minkina, C. Keswani, K. Bauddh, Unravelling the recent developments in the production technology and efficient applications of biochar for agro-ecosystems, Agriculture 13 (2023) 512.

[110] B. Bhatt, S.K. Gupta, S. Mukherjee, R. Kumar, A Comprehensive review on biochar against plant pathogens: Current State-of-the-art and Future Research Perspectives, Heliyon (2024).

[111] W.M. Semida, H.R. Beheiry, M. Sétamou, C.R. Simpson, T.A. Abd El-Mageed, M.M. Rady, S.D. Nelson, Biochar implications for sustainable agriculture and environment:

A review, South African J. Bot. 127 (2019) 333–347.

[112] S. Pérez-Rodríguez, O. Pinto, M.T. Izquierdo, C. Segura, P.S. Poon, A. Celzard, J. Matos, V. Fierro, Upgrading of pine tannin biochars as electrochemical capacitor electrodes, J. Colloid Interface Sci. 601 (2021) 863–876.

[113] D. Van Thuan, H.L. Ngo, H.P. Thi, T.T.H. Chu, Photodegradation of hazardous organic pollutants using titanium oxides-based photocatalytic: A review, Environ. Res. 229 (2023) 116000.

[114] G. Balmuk, M. Videgain, J.J. Manyà, G. Duman, J. Yanik, Effects of pyrolysis temperature and pressure on agronomic properties of biochar, J. Anal. Appl. Pyrolysis 169 (2023) 105858.

[115] X. Cheng, L. Liang, J. Ye, N. Li, B. Yan, G. Chen, Influence and mechanism of water matrices on H2O2-based Fenton-like oxidation processes: A review, Sci. Total Environ. (2023) 164086.

[116] E. Salama, K. Mensah, M. ElKady, H. Shokry, M. Samy, Effective degradation of tetracycline via persulfate activation using silica-supported zero-valent iron: Process optimization, mechanism, degradation pathways and water matrices, Environ. Sci. Pollut. Res. 30 (2023) 87449–87464.

[117] M. Pavel, C. Anastasescu, R.-N. State, A. Vasile, F. Papa, I. Balint, Photocatalytic degradation of organic and inorganic pollutants to harmless end products: assessment of practical application potential for water and air cleaning, Catalysts 13 (2023) 380.

[118] D. Kumar, O.P. Dhankher, R.D. Tripathi, C.S. Seth, Titanium dioxide nanoparticles potentially regulate the mechanism (s) for photosynthetic attributes, genotoxicity, antioxidants defense machinery, and phytochelatins synthesis in relation to hexavalent chromium toxicity in Helianthus annuus L., J. Hazard. Mater. 454 (2023) 131418.

[119] H. Yuan, H. Sun, Y. Shi, J. Wang, A. Bian, Y. Hu, F. Guo, W. Shi, X. Du, Z. Kang, Cooperation of carbon doping and carbon loading boosts photocatalytic activity by the optimum photo-induced electron trapping and interfacial charge transfer, Chem. Eng. J. 472 (2023) 144654.

[120] N.R. Reddy, P.M. Reddy, N. Jyothi, A.S. Kumar, J.H. Jung, S.W. Joo, Versatile TiO2 bandgap modification with metal, non-metal, noble metal, carbon material, and semiconductor for the photoelectrochemical water splitting and photocatalytic dye degradation performance, J. Alloys Compd. 935 (2023) 167713.

[121] X. Su, X. Wang, Z. Ge, Z. Bao, L. Lin, Y. Chen, W. Dai, Y. Sun, H. Yuan, W. Yang, KOH-activated biochar and chitosan composites for efficient adsorption of industrial

dye pollutants, Chem. Eng. J. 486 (2024) 150387.

[122] S. Dong, Y. Gong, Z. Zeng, S. Chen, J. Ye, Z. Wang, D.D. Dionysiou, Dissolved organic matter promotes photocatalytic degradation of refractory organic pollutants in water by forming hydrogen bonding with photocatalyst, Water Res. 242 (2023) 120297.

[123] K. Mishra, N. Devi, S.S. Siwal, V.K. Gupta, V.K. Thakur, Hybrid semiconductor photocatalyst nanomaterials for energy and environmental applications: fundamentals, designing, and prospects, Adv. Sustain. Syst. 7 (2023) 2300095.

[124] R. Xu, J. Li, G. Sui, Y. Zhuang, D. Guo, Z. Luo, S. Liang, H. Yao, C. Wang, Construction of novel CdS@ CuS/g-C3N4 heterojunctions for efficient visible light-driven photo-Fenton degradation performance, Colloids Surfaces A Physicochem. Eng. Asp. 659 (2023) 130598.

[125] R. Chen, S. Ding, N. Fu, X. Ren, Preparation of a g-C3N4/Ag3PO4 composite Z-type photocatalyst and photocatalytic degradation of Ofloxacin: degradation performance, reaction mechanism, degradation pathway and toxicity evaluation, J. Environ. Chem. Eng. 11 (2023) 109440.

[126] S. Lotfi, M. El Ouardi, H.A. Ahsaine, A. Assani, Recent progress on the synthesis, morphology and photocatalytic dye degradation of BiVO4 photocatalysts: A review, Catal. Rev. 66 (2024) 214–258.

[127] S. Meena, M. Sethi, S. Saini, K. Kumar, P. Saini, S. Meena, S. Kashyap, M. Yadav, M.L. Meena, A. Dandia, Molecular surface-dependent light harvesting and photo charge separation in plant-derived carbon quantum dots for visible-light-driven OH radical generation for remediation of aromatic hydrocarbon pollutants and real wastewater, J. Colloid Interface Sci. 660 (2024) 756–770.

[128] W. Zhu, Y. Yuan, Y. Ma, Charge carrier dynamics of surface back electron/hole recombination in BiVO 4 and TiO 2 photoanodes, Sustain. Energy Fuels 8 (2024) 1077–1084.

[129] O.F. Aldosari, I. Hussain, Unlocking the potential of TiO2-based photocatalysts for green hydrogen energy through water-splitting: Recent advances, future perspectives and techno feasibility assessment, Int. J. Hydrogen Energy 59 (2024) 958–981.

[130] Y. Qi, B. Zhang, G. Zhang, Z. Zheng, T. Xie, S. Chen, G. Ma, C. Li, K. Domen, F. Zhang, Efficient overall water splitting of a suspended photocatalyst boosted by metal-support interaction, Joule 8 (2024) 193–203.

[131] P. Bhanot, S.M. Celin, P. Sharma, S.K. Sahai, A. Kalsi, Comparative Evaluation of

Low-and Medium-Pressure UV Lamps for Photo-degradation of RDX Wastewater, Water, Air, Soil Pollut. 234 (2023) 587.

[132] H.T. Akhtar, M.I. Ilyas, T. Fatima, N. Parveen, M.A. Habib, H. Nawaz, M.U. Amin, M.A. Ashraf, BISMUTH BASED NANO-COMPOSITES& THEIR POTENTIAL APPLICATIONS AS PHOTOCATALYST: A CRITICAL REVIEW ON WASTE WATER TREATMENT, (n.d.).

[133] V. Soni, A. Sudhaik, P. Singh, S. Thakur, T. Ahamad, V.-H. Nguyen, L.-A.P. Thi, H.H.P. Quang, V. Chaudhary, P. Raizada, Visible-light-driven photodegradation of methylene blue and doxycycline hydrochloride by waste-based S-scheme heterojunction photocatalyst Bi5O7I/PCN/tea waste biochar, Chemosphere (2023) 140694.

[134] M. Jahani, B.S. Fazly Bazzaz, M. Akaberi, O. Rajabi, F. Hadizadeh, Recent Progresses in analytical perspectives of degradation studies and impurity profiling in pharmaceutical developments: An updated review, Crit. Rev. Anal. Chem. 53 (2023) 1094–1115.

[135] A. Kumar, E. Singh, R. Mishra, S. Kumar, Biochar as environmental armour and its diverse role towards protecting soil, water and air, Sci. Total Environ. 806 (2022) 150444.

[136] J. Chen, P. Wang, L. Ding, T. Yu, S. Leng, J. Chen, L. Fan, J. Li, L. Wei, J. Li, The comparison study of multiple biochar stability assessment methods, J. Anal. Appl. Pyrolysis 156 (2021) 105070.

[137] S. Jha, S. Nanda, B. Acharya, A.K. Dalai, A review of thermochemical conversion of waste biomass to biofuels, Energies 15 (2022) 6352.

Ethical approval

The manuscript has not been submitted to any other journal than this one for simultaneous consideration. The submitted work is self composed and original and has not been communicated for published elsewhere in any language or form (partially or in full). No data, text, or theories by others are presented or communicated anywhere.

Consent to participate and consent to publish

All authors are willing to participate and publish the research article.

Author Contributions

Conceptualization, Supervision, Writing - review & editing: Ajay Kumar. Writing - original draft: Pooja Dhiman, Investigation & Validation: Manisha Dhiman. Formal analysis: Suman Kumari. Data curation: Arush Sharma. Visualization; Writing - review & editing: Manita Thakur

Funding

The authors declare that no funds, grants, or other support were received during the preparation of this manuscript

Competing Interests

The authors declare that they have no known competing financial interests or personal relationships that could have appeared to influence the work reported in this paper.

Table 1: Biochar prepared from different feedstock by slow pyrolysis

	Feed Stock	**Reagent**	**Operating Temperature(°C)**	**Residence Time (Hrs)**	**Heating Rate (°C/min)**	**Characteristics**	**Ref.**
Slow Pyrolysis	Pine Bark	Co(NO$_3$)$_2$. 6H$_2$O and Fe (NO$_3$)$_3$ .9H$_2$O	950	2	30	Magnetic biochar were well crystallined with spinel-type lat- tice of cobalt ferrite	(Kermannezhad et al. 2024)
	Date Pits	FeCl$_3$	700	1	10	Biochar with Bet surface area 780.06m^2/g	(Gotore et al. 2024)
	Cotton wood	AlCl$_3$ .6H$_2$O	600	1	-	biochar possessed rough,	(Khan et al. 2024)

					porous morphology owing to the intrinsic nature of the biochar matrix	

Table 2: Biochar synthesized from different biomass by Fast pyrolysis

Fast Pyrolysis	**Feed Stock**	**Operating Temperature (^{o}C)**	**Residence Time(min)**	**Heating Rate (degree /Min)**	**Characteristics**	**Ref.**
	Sugarcane bagasse	600	-		-	(Zafeer et al. 2023)
	Corn cob	275	60 min		Biochar with low surface area and coarse particle distribution	(Varela et al. 2024)
	Eucalyptus grandis	700 500	3-70 min < 2 sec	>100	Bio-oil is obtained	(Porto et al. 2024)
	cellulose, lignin and hemicellulose	~500°C Short hot vapour residence time	Upto 10 sec	-	75 wt% (bio-oil)+12 wt%+char 13 wt%	(Sharma et al. 2024)

Table 3: Biochar generated from biological feedstock by Flash pyrolysis

	Feed Stock	**Operating Temperature**	**Residence Time**	**Heating Rate**	**BET and Porosity**	**Characteristics**	**Ref.**
Flash Pyrolysis	Pine wood	1405-1667 K	<0.1Sec	10^5 K/sec	0.684	Bio-oil	(Chuanchai and Wu 2024)
	Beech Wood(flash liquid + Gas)	>925°C	<1 sec	High	-	Bio-oil, chemicals and gas	(Tagne et al. 2022)
	Birch (Betula pendula) wood	700°C	4 hrs	high	-	-	(Rusanen 2021)
	Biomass	450–600°C	<1 Sec	10^3–10^4	-	Bio-fuel with higher water content (>15%) underwent re-polymerized, unstable, and hydrocarbon immiscible.	(Zayoud et al. 2022)

Table 4: Biochar based adsorptive elimination of heavy metals

Raw Feedstock	**Temp. (°C)**	**Residence Time (min)**	**Heavy metal contaminant**	**metal surface area (m^2 g^{-1})**	**Adsorption capacity (mg g^{-1})**	**Literature**
Manure of pig	700	120	Cu (II)	73.49	9.09	(Shen et al. 2020)

Straw of corn	700	120	Cd(II)	13.10	73.32	(Zhou et al. 2021b)
Cauliflower leaves	600	120	Cu (II)	12.50	75.99	(Ge et al. 2020)
Straw of Sesame	700	240	Cd(II)	289.20	86.00	(Zhou et al. 2020)
Miscanthus sacchariflorus	600	60	Cd(II)	381.50	17.23	(Pidlisnyuk et al. 2021)
Pinewood sawdust	700	120	Cu (II)	419.10	8.9	(Gope and Saha 2021)
husk of Rice	700	120	Cd(II)	242.53	93.50	(Saeed et al. 2022)
Alternanthera philoxeroides	600	180	Pb(II)	19.79	53.71	(Wang et al. 2022b)
straw of Rice	700	240	Cd(II)	161.18	65.40	(Xu et al. 2022)
Peanut hull AC	220	12 hrs	Cr(VI)	101.01	142.86	(Luo et al. 2023a)

Table 5: Utilization of Biochar supported photo-catalysts in removal of dyes from waste water discharged from textile industries

Composite	**Feedstock**	**Dye Pollutant**	**Light source and wavelength(nm)**	**Surface area (m2 g− 1)**	**Degradation efficiency**	**Reusability % (cycle**	**Reference**
Biochar-g-C$_3$N$_4$	L(+)-arginine, and puree Urea, glycine,	Orange-G(OG)	15 W, UV 380 nm	-	98.83	-	(Faheem et al. 2020)

AlBcTNC (Algal biochar reinforced trimetallic nanocomposite)	Algae	Malachite Green(MG)	Solar light	107.2	94	94 (Fifth cycle)	(Kumar et al. 2023a)
ZnO/JFC char from Jute fibers	Jute Fibre	Methylene Blue(MB)	UV light 320–400 nm	4.71	99	80 (7th cycle)	(Yu et al. 2021)
Biochar-ZnO	Pecan nutshells	Reactive Red-97(RR-97)	UV lamp, mercury-vapor 18 W	253.23	82.64	90 (9th cycle)	(Leichtweis et al. 2020)
WFB/BiOBr	Wood flour	Rhodamine B(RhB)	200 W LED lamp	222.39	-	-	(Sutar et al. 2022)
ZnO@RSDBC -biochar derived from Rectorite-sludge	Rectorite sludge	Acid Orange-7(AC-7)	100 W visible light lamp 485 nm	15.54	93.8	78.6 (3rd cycle)	(Sutar et al. 2022)
BC-6	Corn cob	Methyl orange (MO)	Visible light	468.59	86.41	3rd cycle	(Pang et al. 2021)
TiO_2/BC	Coconut Shell	Reactive Brilliant Blue KN-R	300 W, UV light xenon lamp	7.21	99	73.98 (5th cycle)	(TURKTEN and KARATAS 2023)

Bi$_5$O$_7$I/TWB/PCN(40 wt%)	Tea waste	Methylene Blue (MB)	300 W halogen lamp	7	92.02 92.02% (MB)/60 min,	88, (4th cycle	(Soni et al. 2023)
WO$_3$@TiO$_2$/CS-biochar	Polysaccharide chitosan biochar (CS-biochar)	Methylene Blue (MB)	500 W Xe lamp (λ > 400 nm)	46.20	97.2	Good stability with reproducibility	(Feng et al. 2023)
CuS–Mg/S-BC	Bagasse	Rhodamine(RhB)	simulated solar light irradiation	588.07	95.70	inferior adsorption-photocatalytic durability after 7th cycle	(Liu et al. 2024)
biochar/NiCr-LDH	Walnut shells	Methyl orange(MO)	500 W Xe lamp, 464 nm	51.45	98.18	Good recycling stability	(Li et al. 2023b)
SnS$_2$/BC	Areca nut shells	Congo Red(CR)	23 W LED light with 11,790 lx with radiation intensity of 50.67 W m^{-2} at ~32°C	78.01	98.43	80, 4th cycle	(Gadore et al. 2023)

70% BiOBr/BC	Bamboo	Reactive red 120 (RR120)	Simulated light under modified Elovich models	11.62	70	Very stable(3^{rd} cycle)	(Luo et al. 2022)

Table 6: Utilization of Biochar photocatalysts in removal of phenolic compounds from water bodies

Composite	**Feedstock**	**Phenolic compound pollutant**	**Light source and wavelength(nm)**	**Surface area (m^2 g^{-1})**	**Degradation efficiency**	**Reusability % (cycle**	**Reference**
g-C_3N_4/$FeVO_4$/biochar	Needles of pinus	Methylparaben and chlorophenol	-	192.5	90.1 and 85.3	97.4 and 89.1 (Sixth cycle)	(Kumar et al. 2017)
TiO_2/Biochar	Softwood pellets	Phenol	125 W mercury lamp with 365 nm	254	64.1	64(Fifth cycle)	(Shukla et al. 2021)
$CoFe_2O_4$/Ag_3PO_4	Pollens of pine	Bisphenol A	300 W Xe lamp with ≥420 nm	-	91.21	90(Fifth cycle)	(Zhai et al. 2020)
g-C_3N_4/biochar	Corn straw	Naphthalene	200 W high-pressure sodium	-	82.19	99 (Fifth cycle)	(Ali et al. 2022)

			lamp with 400–800 nm				
Bi/Bi$_2$O$_3$/Biochar	Rice straws	Estrone	500 W Xenon lamp with 350–700 nm	338.2	94.7	82.9 (5th cycle)	(Zhang et al. 2021)
Ag$_3$PO$_4$/Fe$_3$O$_4$ - activated biochar	Bamboo particles	Bisphenol A	250 W LED lamp with 450 nm	4.28	95.6	-	(Talukdar et al. 2020)
Carbon nitride(Polymeric)/BC	Corn Cub	Bisphenol A	300 W xenon lamp with 420 nm	-	97.23	-	(Wang et al. 2021)
Co(II)-BiOCl@ BC nanosheets	Sludge	p-nitrophenol	Mercury lamp (254 nm)	-	99.4	89.82 (Fifth cycle)	(Wang et al. 2023)
ZnO/BC	Cellulose nanocrystals	Phenol	125 W mercury lamp UVirradiation	-	99.8	69 (Fifth cycle)	(Sutar et al. 2022)
TiO$_2$/BC	Rice husk	Bisphenol-A	UV light with 30 W, UV lamp	821	>89	77(Eighth cycle)	(Van Thuan et al. 2023a)

Table 7: Utilization of Biochar supporterd photocatalysts in removal of pharmaceutical pollutants from waste water

Composite	**Feedstock**	**Pharmaceutical Pollutant**	**Light source and wavelength(nm)**	**Surface area (m^2 g^{-1})**	**Mineralization efficiency**	**Reusability % (cycle**	**Reference**
TiO_2-Biochar	Corn cob	Sulfamethoxazole	UV lamp with λ 254 nm	383	91	-	(Minaei et al. 2024)(Inyang and Dickenson 2015)
TiO_2-Biochar	Reed straw	Sulfamethoxazole	50 W xenon lamp (UV irradiation)	102.16	91.27	86 (Fifth Cycle)	(Sherpa et al. 2024)(Yadav et al. 2023)
Fe_3O_4/BiOBr /Biochar	Reed straw	Carbamazepine	50 W Visible LED	26.41	95.51	90.15 (Fifth Cycle)	(Penghui et al. 2022)
CdSe quantum dots/Biochar	Bamboo	Tetracycline	250 W Xe Lamp with λ 420 nm		82.6	99.6 (Fourth Cycle)	(Sutar et al. 2022)
Zn–Co-LDH@Biochar	Wheat husks and paper sludge	Gemifloxacin	10 W UV-B light (UV irradiation)	95.76	92.7	90 (Fifth Cycle)	(Gholami et al. 2020)
TiO_2–KBiochar	Cornstalk	Enrofloxacin	15 W UV lamp	36.65	85.25	77.14 (Fifth Cycle)	(Sutar et al. 2022)

			with λ 254 nm				
Ball milled Biochar	Poplar woodchips	Enrofloxacin	500 W Xe lamp (Visible light irradiation)	151	80.2	-	(Xiao et al. 2021)
$CuWO_4$ NCs–BC	Neem leaves	Ciprofloxacin	Tungsten lamp λ >400 nm	6.81	97	79 (Fifth Cycle)	(Li et al. 2022c)(Mishra et al. 2023a)
BC/BiOCl nanosheet	Bamboo leaves	Tetracycline	300 W Xe lamp with λ 200–800 nm	35.97	71.8	70 (Fifth Cycle)	(Jalal et al. 2023)
Graphitic carbon nitride (gC_3N_4)/Biochar	Poplar woodchips	Enrofloxacin	500 W Xe lamp (UV irradiation)	2.68	81.1	55.3 (Fourth Cycle)	(Grist et al. 2022)
Bi_2WO_6/Fe_3O_4/Biochar	Reed straw	Ofloxacin and Ciprofloxacin	50 W LED lamp λ 475 nm	24.48	83.1 and 91.5	99.85, 86.65 (Fifth Cycle)	(Maddi et al. 2023)
MnFe-LDO–Biochar	Palm seed	Metronidazole	9–30 W, T8, (UV irradiation)	524.8	97	88 (Third Cycle)	(Azalok et al. 2021)
Biochar/BiOBr	Straw	Ciprofloxacin	500 W xenon lamp	-	96.8	85 (Fourth Cycle)	(Jalal et al. 2023)

Perylene diimide/BC	Rice straw	Iohexol	250 W Xe Lamp with λ >420 nm	-	100	-	(Grist et al. 2022)]
$ZnAl_2O_4$/Lychee/BC	Lychee-biochar	Ibuprofen(IB)	-	111.69	100	stable , active for six reuse cycles	(Maddi et al. 2023) (Maddi et al. 2023)
Bi_5O_7I/TWB/PCN	Tea waste	Doxycycline hydrochloride	300 W halogen lamp	7	90.21	Excellent stability after Fourth cycle	(Ke et al. 2022)
WO_3@TiO_2/CS-biochar	polysaccharide chitosan biochar (CS-biochar)	Tetracycline(TC)	500 W Xe lamp with λ > 400 nm	46.20	97.2	Good stability with reproducibility	(Feng et al. 2023)
NiAl-LDH/Biochar-0.5	Bamboo	Tetracycline(TC)	300 W Xe lamp (PLS-SXE300+, Perfect light with λ 356 nm	124.2	94.4	-	(Rohmatullaili et al. 2024)
PbMoO4@Biochar (PBC)	Poplar sawdust	Teracycline(TC)	300w Xe lamp with λ 360 nm	20.10	52.68	High stability after	(Jiang et al. 2023)

						Fifth cycle	
Cu$_2$O/SCG@ biochar	Spent coffee grounds	Sulfamethoxazole (SMX)	xenon lamp (500 W), with λ 420 nm	-	80	-	(Zheng et al. 2022)
SnS$_2$/biochar	Areca nut shells	Amoxicilline(AM)	23 W LED light with 11,790 lx and radiation intensity of 50.67 W m^{-2} at ~32°C	78.01	93.72	80, Fourth cycle	(Gadore et al. 2023)

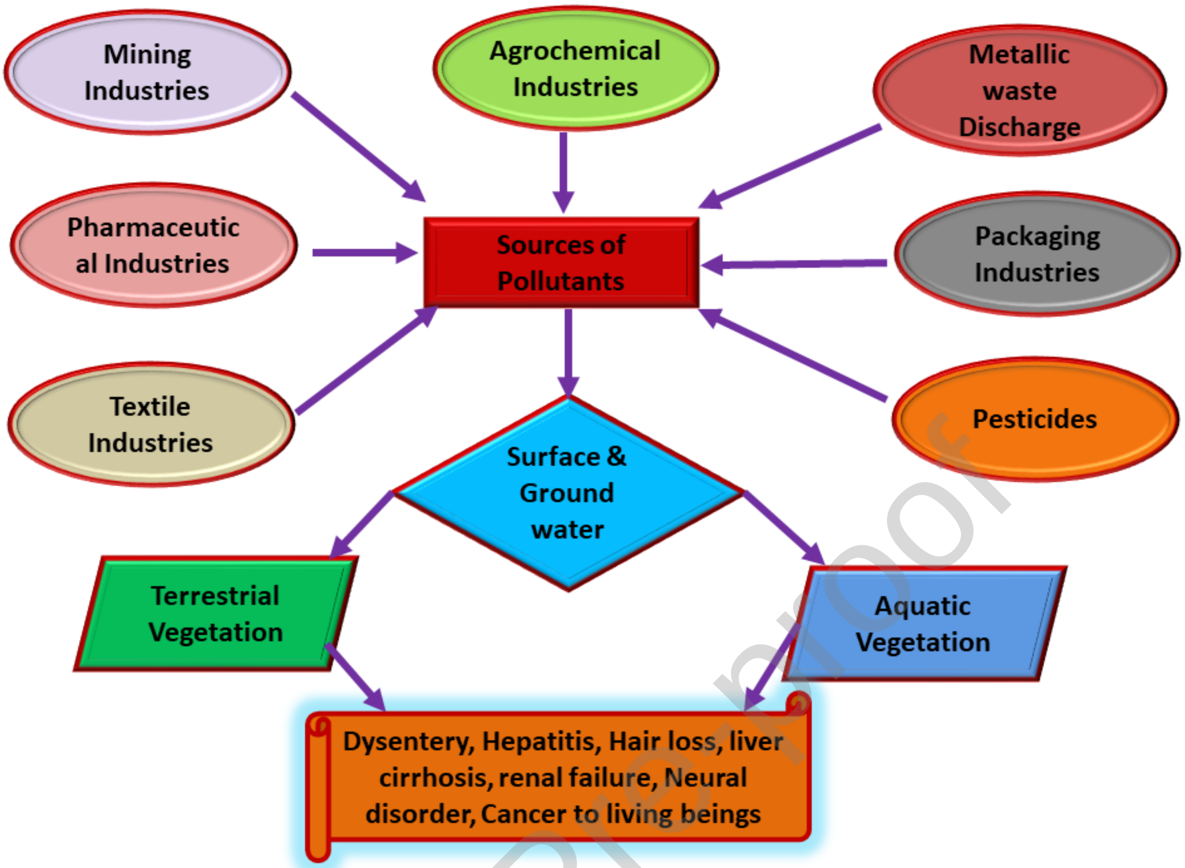

Figure 1: Different Sources of Industrial Pollutants

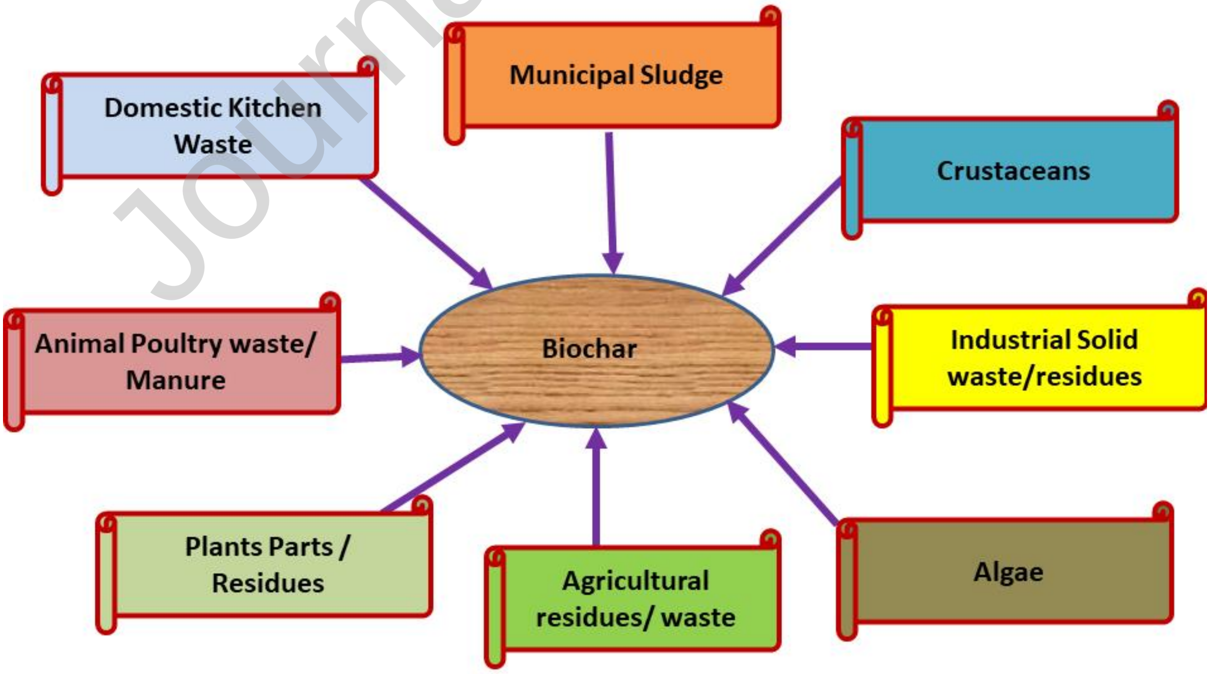

Figure 2: Different Sources of Biomass Feedstock for Biochar Production

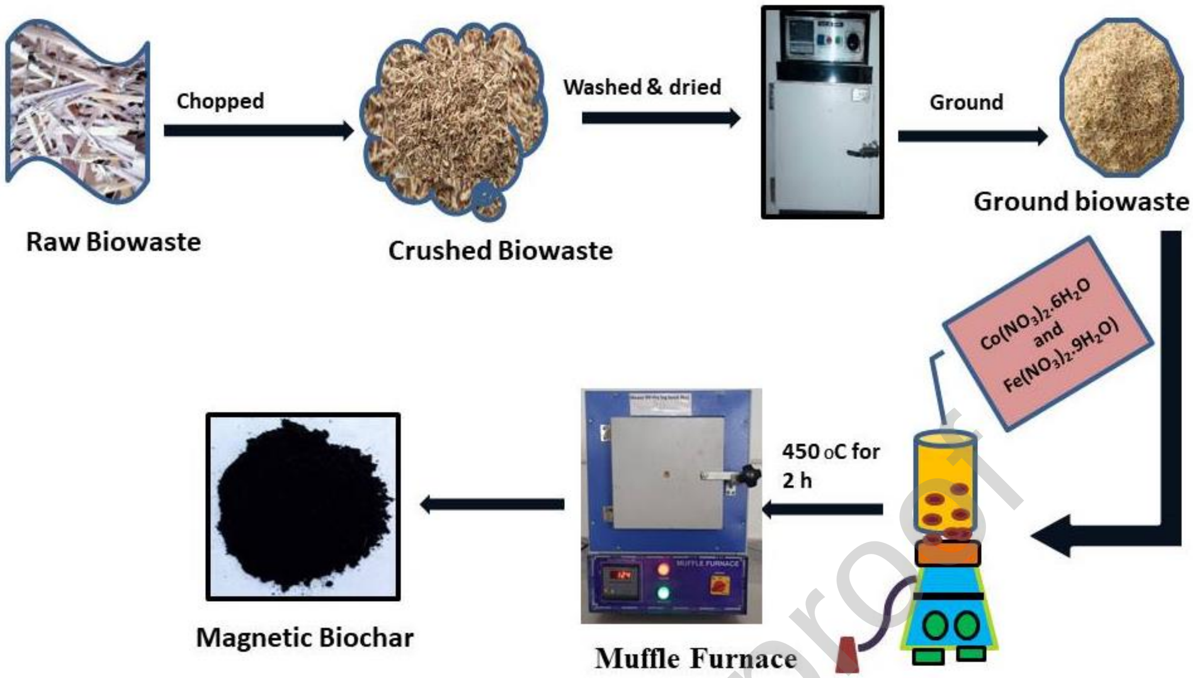

Figure 3: Magnetic Biochar Synthesis from Different Bio-Waste

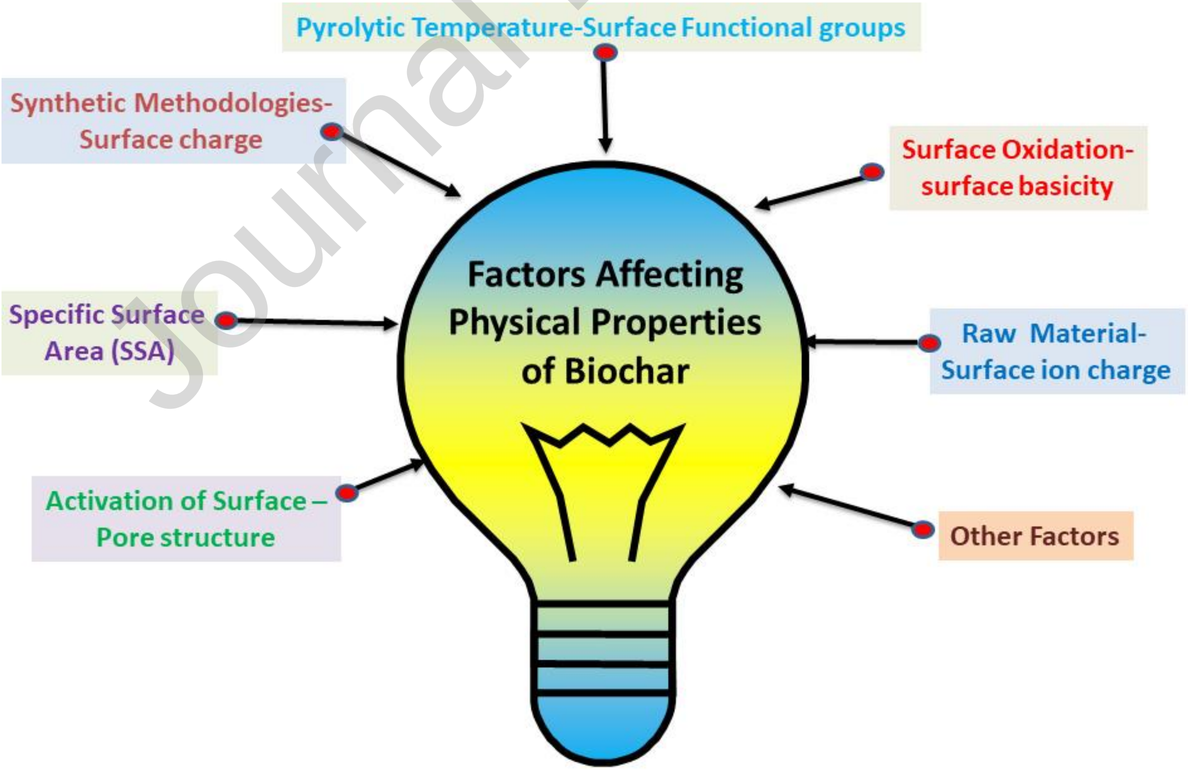

Figure 4: Illustration of the Factors Affecting Physical Properties of Biochar

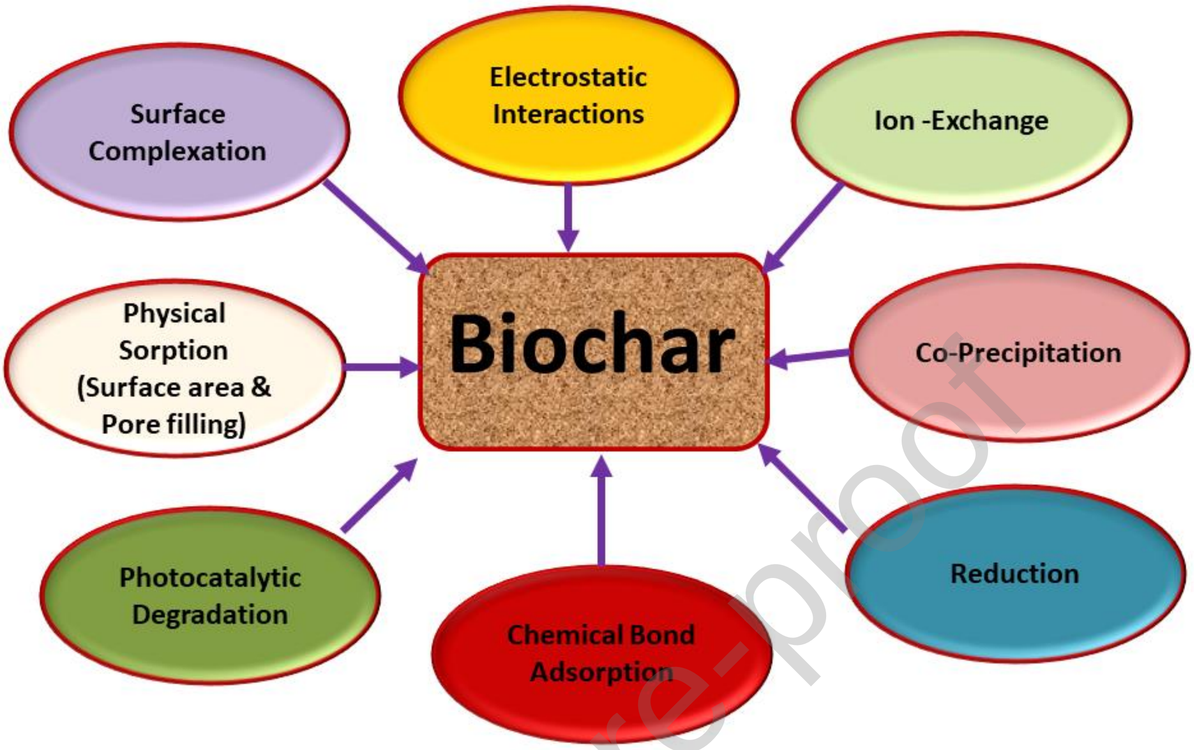

Figure 5: Schematic Diagram Illustrating Different Physical Mechanism for elimination of Organic Pollutants from Waste Water

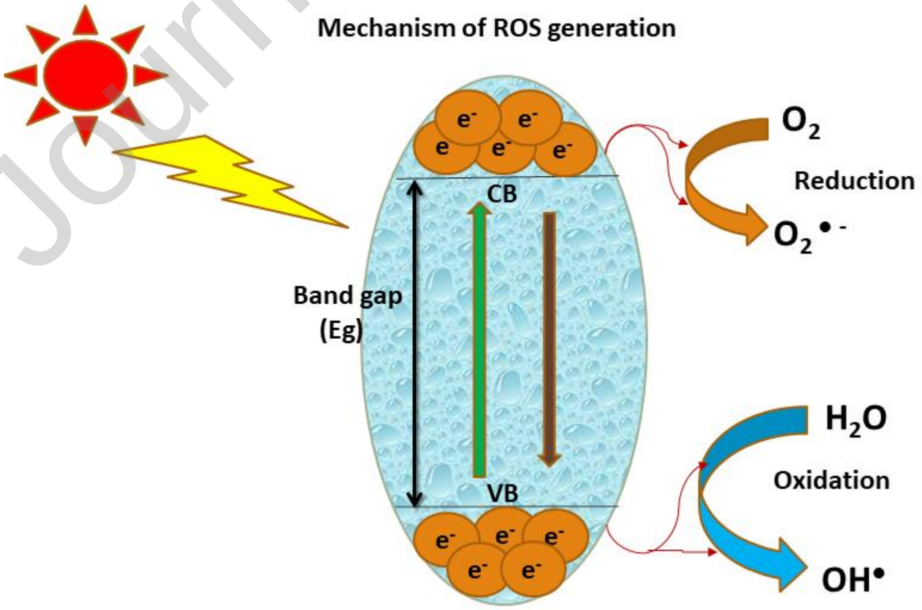

Figure 6: Schematic Diagram of the Mechanism of Photo-catalysis

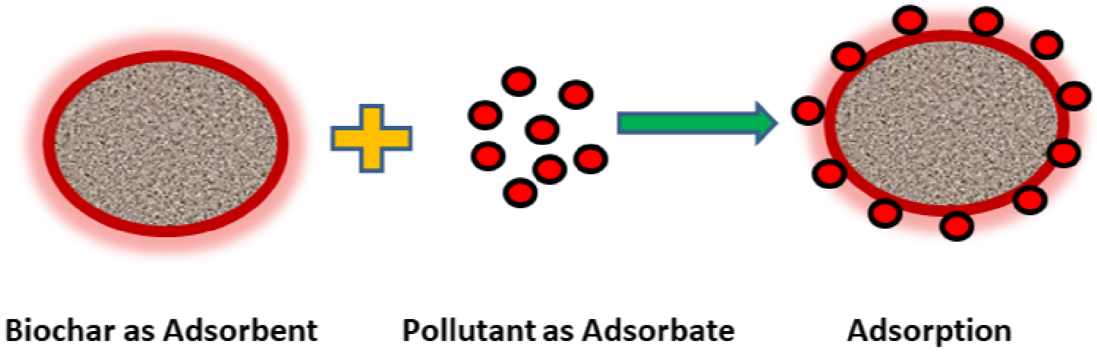

Figure 7: Brief Description of Adsorption Process

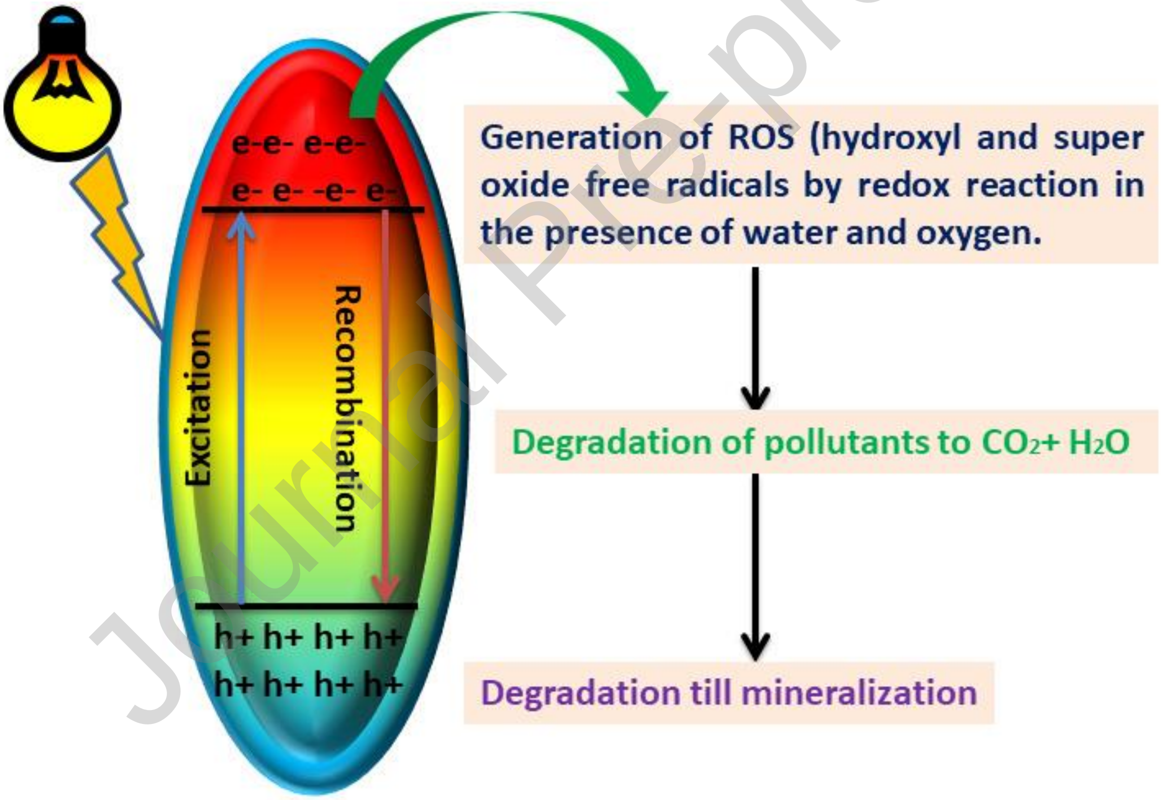

Figure 8: Brief Mechanism of Adsorption led Photo-catalytic Degradation Process

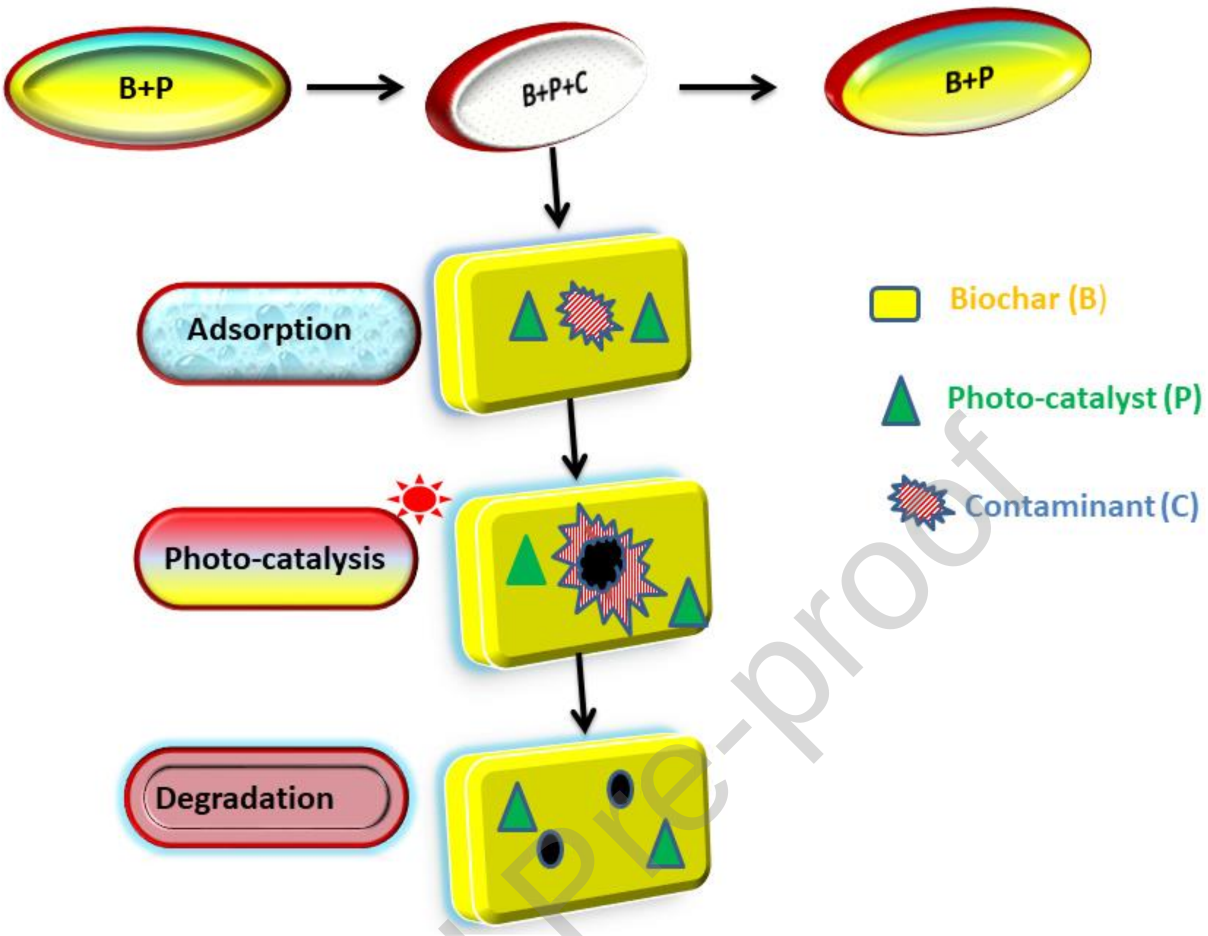

Figure 9: Adsorption cum photo-catalytic degradation of organic pollutants

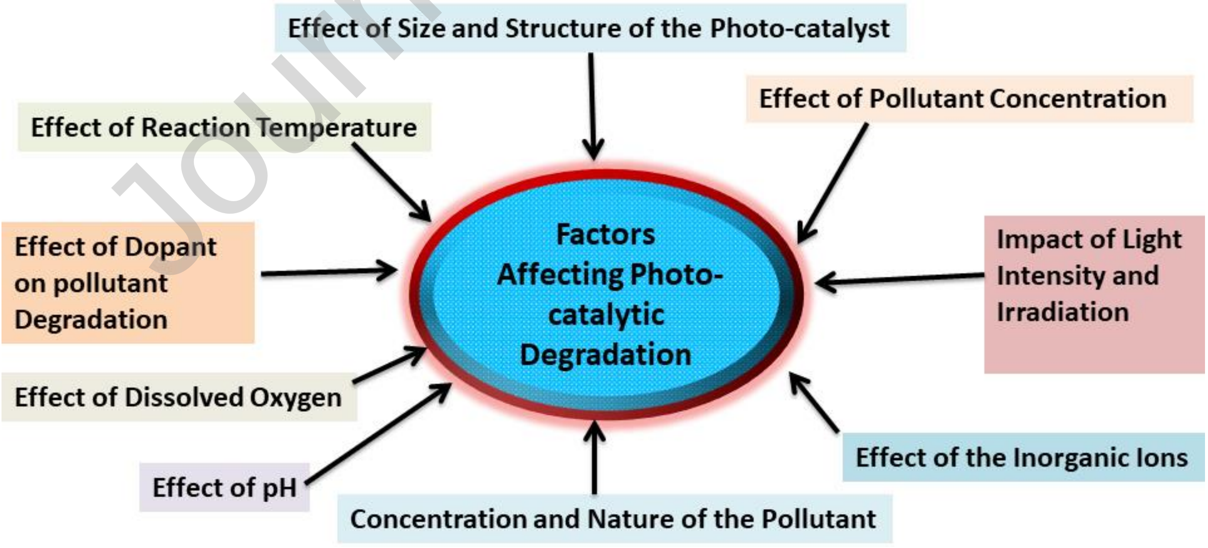

Figure 10: Illustrating the Different Factors Affecting Photo-Catalytic Degradation

Declaration of interests

☒ The authors declare that they have no known competing financial interests or personal relationships that could have appeared to influence the work reported in this paper.

☐ The authors declare the following financial interests/personal relationships which may be considered as potential competing interests: